AMBIENT AND ELEVATED TEMPERATURE MECHANICAL BEHAVIOR OF A HIGH STRENGTH ALUMINUM ALLOY AFTER COLD DEFORMATION

A Thesis

by

Kambiz Shojaei

Submitted to the
Graduate School of Sciences and Engineering
In Partial Fulfillment of the Requirements for
the Degree of

Master of Science

in the
Department of Mechanical Engineering

Özyeğin University
January 2016

AMBIENT AND ELEVATED TEMPERATURE MECHANICAL BEHAVIOR OF A HIGH STRENGTH ALUMINUM ALLOY AFTER COLD DEFORMATION

Approved by:

Assist. Prof. Dr. Güney Güven Yapıcı
Advisor
Department of Mechanical Engineering
Özyeğin University

Assist. Prof. Dr. Kadri Can Atlı
Department of Mechanical Engineering
Anadolu University

Assist. Prof. Dr. Zeynep Başaran
Department of Civil Engineering
Özyeğin University

Date Approved: 11 January 2016

To the reasons of my happiness, To my family

ABSTRACT

Nowadays, aluminum alloys in automotive and aerospace industries have assigned a noticeable portion in structural applications in comparison to many steel alloys. The aim of this study was to investigate the high temperature deformation behavior and microstructural evolution of Al-Zn-Mg-Cu aluminum alloy for two different annealed and cold rolled conditions. The elevated temperature deformation behavior and microstructural evolution of 7075 aluminum alloy at the annealed and cold rolled conditions have been studied. Isothermal uniaxial tensile tests at different temperatures of ambient temperature, 200, 250, 300 and 350 °C and strain rates of 0.001, 0.01, 0.1 s^{-1} were conducted.

The effects of two important factors; deformation temperature and strain rate sensitivity on the tensile deformation behaviors with support of fracture mechanism characteristics are discussed in details. The Zener-Hollomon parameter in an exponent-type equation has been utilized for both tested conditions in order to calculate the activation energy for the studied conditions. The results review indicates that with the increase of deformation temperature or the decrease of strain rate, the fraction of recrystallized grains increases which leads to higher elongation. This is mainly attributed to dynamic recrystallization during the tensile deformation. Accordingly, the maximum UTS value at elevated deformation temperature has been reported 218 MPa in rolled samples at 200 °C under the strain rate of 0.1 s^{-1}, whereas the maximum elongation to fracture was 55.9% in rolled samples at 350 °C under the strain rate of 0.01 s^{-1}.

In addition, unlike annealed condition it has been observed that the cold working

has a remarkable effect on increasing the peak stress and also leads to higher ductility at elevated deformation temperatures. But in contrast, at ambient temperature it has been observed that severely cold work could decrease the ductility. However, at 350 °C and 0.001 s^{-1} the general trend of softening has changed and the ductility dropped which could be imputed to the dynamic precipitation resulting in the formation of the secondary phases during high temperature deformation. Observation of the fracture surfaces in the studied deformation conditions has showed that localized necking caused the final fracture of the specimens in which microvoids can be seen at lower deformation temperatures. Whereas by increasing the deformation temperature coalescence of dimples and micro voids leading to a relatively coarse but less dense morphology resulted in fracture.

Keywords: Al-Zn-Mg-Cu alloy, High temperature deformation, Cold work, Fracture morphology, Activation energy, Mechanical behavior

ÖZETÇE

Günümüzde alüminyum alaşımların çelik alaşımlara oranla otomativ ve uzay sanayisinin yapısal uygulamalarında daha fazla tercih edildiği görülmektedir. Bu tezde 7075 alüminyum alaşımının tavlanmış ve haddelenmiş durumları altında sıcak şekil değiştirme karakteristiği ve mikro yapısal gelişimi incelenmiştir. Test numuneleri üzerinde farklı çevresel sıcaklıklarda (200, 250, 300 ve 350 °C) ve farklı gerinme oranlarında (0.001, 0.01, 0.1 s^{-1}) izotermik tek eksenli çekme testleri gerçekleştirilmiştir.

Test sonuçları üzerinde iki önemli etken olan sıcaklık ve gerinme oran duyarlılığı kırılma mekanizmaları desteği ile tartışılmıştır. Test edilen durumların aktivasyon enerjilerinin hesaplanabilmesi için örnek denklemlerdeki Zener-Hollomon değişkeninden faydanılmıştır. Yapılan testlerin sonucunda deformasyon sıcaklığındaki artışın ya da gerinim oranlarındaki azalışın yeniden kristalleşmiş tane oranını arttırdığı görülmüştür. Bu artışın daha fazla uzamaya olanak sağladığı anlaşılmıştır. Bu durumun sebebi olarak çekme deformasyonu sırasındaki dinamik yeniden kristalleşme öngörülmüştür. Dolayısıyla, 200 °C ve 0.1 s^{-1} gerinme oranındaki haddelenmiş numunelerin maksimum UTS değeri 218 MPa olarak ölçülmüştür. Oysa ki 350 °C ve 0.01 s^{-1} gerilme oranına sahip haddelenmiş numunelerin kırılmaya kadar uzama oranı 55.9% olarak ölçülmüştür.

Ayrıca tavlamanın aksine soğuk işlemelerin maksimum gerilme değerini arttırdığı ve bu durumunda yüksek deformasyon sıcaklıklarından daha fazla sünekliğe yol açtığı görülmüştür. Tam tersine, ortam sıcaklığında soğuk işlemelerin esnekliği azalttığı gözlemlenmiştir. Ancak 350 °C sıcaklık ve 0.001 s^{-1} gerinme oranında genel yumuşama

eğiliminin geliştiği ve sünekliğinin azaldığı görülmüştür. Bu azalış yüksek sıcaklıklardaki deformasyon esnasında oluşan ikincil evrelerdeki dinamik çökelme ile açıklanmaktadır. Çalışılan şekil değiştirme şartlarında incelenen kırılma yüzeyleri ile numunelerde düşük sıcaklık kırılmalarına mikro boşlukların bulunduğu bölgesel boyun vermelerin sebep olduğu anlaşımıştır. Öte yandan, sıcaklığın artması ile boşlukların birleşmesi sayesinde kırılma meydana gelmiş olup, daha iri ve fakat düşük yoğunluğa sahip bir kırılma morfolojisi ortaya çıkmıştır.

ACKNOWLEDGEMENTS

Like a cheerful moment at the finish line of a run that makes you feel think to all those efforts you have undertaken to finish it up, this thesis owes its existence to the help, support and inspiration of several people. Firstly, I would like to give my sincere gratitude to my advisor, **Dr. Guven Yapici**; his support, encouragement and advises smoothed away difficulties I had along my research work. Many thanks to **Dr. Duygulu**, **Dr. Zeytin** and all the researchers at TUBITAK Marmara Research Center Materials Institute lab. They provided me technical assists and help for microstructural studies.

I would like to also thank **Mr. Ulas Yildirim** and **Vahid Sajjadifar** for their supports and assists in manufacturing, practical and scientific parts of my project. Besides from their supports, they were like my big brother since the first day I came to Ozyegin. Many thanks to all my colleagues and office mates, **Sabri Orcun Orhan**, **Gorkem M. Simsek**, **Ali Vahid-Yeganeh**, **Cagla Akcay** and **Salar Salahi**. Their support and encouragement was a key point for me to overcome the difficulties throughout this way. I would like to also offer my kindest gratitude to a valuable friend of mine, **Mostafa Motahari**, for his sincerer help and friendship. I was so fortunate to have a chance to work at **MEMFIS** research group over past three years of my academic life with all these great people in such a friendly and professional atmosphere. Special thanks goes to my old university friend, **Mani Rostampour**, who is now living in Tehran for all of his supports and encouraging messages all day and night that kept me motivated. I would like to also thank one of my best friends, **Cem Gunes** for all his kindness to me and he knows exactly what I mean.

Many thanks to **Strava**, my running app that inspired me to shiver out all of

my stresses and kept me smiling and positive in those down days of my life. Special thanks goes to my special brother, **Koorosh**. Defiantly, he was the biggest happiness of my life in Istanbul over the past three years.

The last but the most importantly, I would like to express my deepest gratitude to my beloved **Father** and **Mother** for their love and unconditional supports. You made me live the most I loved to and that has made me who I am now.

TABLE OF CONTENTS

LIST OF TABLES

LIST OF FIGURES

CHAPTER I

INTRODUCTION

1.1 Background

Aluminum alloys are being used in engineering structures more than every other time. This attraction has increasingly merged to vast range of applications by investigating of researchers on its processing-microstructure, thermomechanical properties and inter-relations which leads to a comprehensive understanding of the material's behavior [3, 4]. Among all different types of aluminum alloys, the 7xxx series (Al-Zn-Mg-Cu alloy) are superior, due to their high strength, low density, excellent stress corrosion resistance and fracture toughness; and perform a widespread role in manufacturing semi-finished products that have been used for many structural parts in aerospace industries [5–8].

Moreover, in automotive industries, the tendency to manufacture lighter vehicles and at the same time a fuel efficient one has led to noticeable interest in replacing steel with aluminum alloys. However, conventional stamping of aluminum alloys into sheet metal parts is limited by their low formability as compared to steel sheet [9]. To be able to somehow compensate this gap, superplastic forming is one of the conventional methods to produce aluminum parts with high complexity and deep curvature surfaces.

Besides, characterizing the plastic deformation properties and grain structure evolution during high temperature deformation need to be studied to reach high strength and fracture toughness. Selecting the zinc-magnesium-copper aluminum alloy 7075 as objective material has made us to investigate on the thermomechanical processing condition of this alloy. Fully heat treated T651-condition, exhibits the highest

strength as far as aluminum is concerned used in commercial structures. Apart from the strength, providing a great formability could be the result of the O-tempered condition in the studied alloy which has been fully annealed. Likewise, to increase the strength of the O-tempered condition, one applicable way is to conduct severe cold working. Thus, investigating the ductility level at both ambient and elevated temperature conditions of the alloy is one of the key objectives of the current research work.

Generally, the description of plastic deformation behavior starts from hot working of metals where the hot deformation temperature range of a metal can be defined as it is above 0.5 T_m where T_m is the absolute melting point of metal in K. There are two main parameters in plastic deformation of a metal which are playing a significant role on its behavior; strain rate and deformation temperature. the improvement in dislocation mobility with increasing temperature T arise from augmented vibration of the atoms.

Normally in metals, the average amplitude of vibration increases to about 10 of the lattice parameter at the absolute melting point (T_m, K) which is characterized as bonding strength of a metal [10]. According to this principle the hot working temperature range of aluminum alloy starts at temperatures above 250 °C, likewise, in the present study the high temperature deformation starts at 2000 °C and with 50°C temperature intervals it is reaching up to 350 °C. For alloys, the T_m of the pure metal is used as the lower limit and in practice rises as the alloying elements impede dislocation motion. The commonly used strain rate $\dot{\epsilon}$ range for industrial mechanical forming is 10^{-3} s^{-1} to 10^{2} s^{-1}; however, there is a possibility of happening creep at the range of $10^{-10} - 10^{-4}$ s^{-1} and traditional tension testing is about $10^{-5} - 10^{-3}$ s^{-1}.

Hot workability of a metallic alloy could consist of low flow stress, high ductility and sound product with properties suitable for the application. A low flow stress could be achieved from increasing deformation temperature or decreasing the strain rate.

High ductility provides larger formability of complicated shapes at higher rates with improved productivity, product quality, and reduced cost for nondestructive testing. If the product is intended for direct service, the final forming condition and cooling rate can be selected to preserve the strength of the hot worked structure [10]. The goal of this research is to optimize the processing conditions for the best combinations of strain rate and deformation temperatures at both ambient and elevated temperatures [10].

In this study we have focused on the elevated temperature deformation of the annealed (O-tempered) and the rolled conditions of the aluminum alloy 7075. Accordingly, a series of isothermal uniaxial tensile tests at different temperature range of ambient temperature, 200, 250, 300 and 350 °C and strain rates of 0.001, 0.01, 0.1 s^{-1} were conducted. The effects of two important factors; deformation temperature and strain rate on the elevated temperature tensile deformation behaviors with support of fracture mechanism characteristics are discussed in details. The Zener-Hollomon parameter in an exponent-type equation has been utilized for both tested conditions in order to calculate the activation energy of the studied conditions.

CHAPTER II

LITERATURE REVIEW

2.1 Aluminum Alloys

2.1.1 The History and Production Process of Aluminum

Aluminum has been identified as the most common metal on earth, shaping about eight percent of the earth's crust. It is also the third most abundant element known to mankind. On top of it, only oxygen and silicon (sand) exist in larger quantities. Back in to 1808 that Sir Humphrey Davy, the British electrochemist, discovered the existence of aluminum, and just 17 years later the Danish scientist Oersted has made the first tiny pellet of the metal. The next step in exploration of aluminum happened this time in Germany by Wohler in 1845 [11].

He established the specific gravity of aluminum that determined one of the fascinating characteristics of aluminum its lightness. He also discovered that it is easy to shape it while it can be melted just with a heat generated by a blow torch. Later on in France, Henri Saint and Clair Deville discovered a production technique that enabled them to display a solid bar of the metal at the Paris Exhibition in 1855. Introducing the new manufacturable metal at that time was a great fortune and great achievement for him that made aluminum more valuable than gold, silver or platinum. Napoleon III became eager to utilize this new metal for his military purposes. To make this happen, he subsidized Deville to find out a productive solution to utilize this metal for mass production [12].

Later on, after many trials had failed to find out a processing solution, in 1886 two scientists, Heroult and Hall had been concerned completely with a chemical process for producing the metal. They believed the cost-efficient production key is in electrolytic

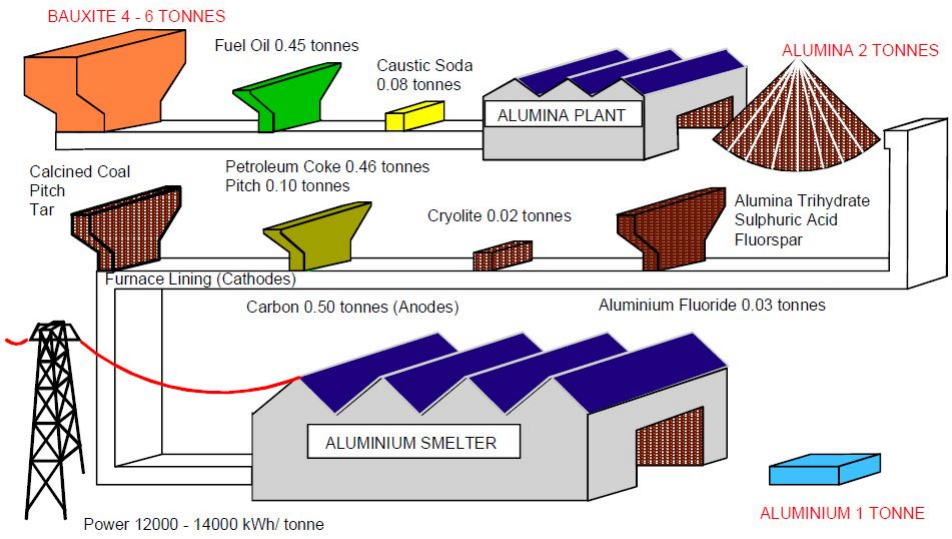

Figure 1: Raw materials to produce a 1 ton of aluminum ingot [1]

method. They had evolved with finding a substance that could by passing through the electricity, the aluminum oxide (alumina) would dissolve and then that could turn out to deposit the aluminum as a metal. Since that day, processing aluminum has undergone massive changes and improved over time so that the today's modern planet needs 12 to 14 kilowatt hours of electricity to dissolve 2 kilograms of alumina to produce 1 kilogram of aluminum. A scaled up of the raw materials to produce a ton of metal is shown in Fig. 1.

2.1.2 Important Physical Properties of Aluminum

Atomic and crystal structure, density, electrical conductivity and resistivity, non-magnetic property, thermal conductivity, reflectance and emissivity, corrosion resistance, thermal expansion, melting temperature, specific latent heats and many more could be considered as important physical properties of aluminum as some features are discussed below.

As a third most abundant element in Earth's crust after oxygen and silicon, it is the most plentiful of all metals. Aluminum has the atomic number of 13 which

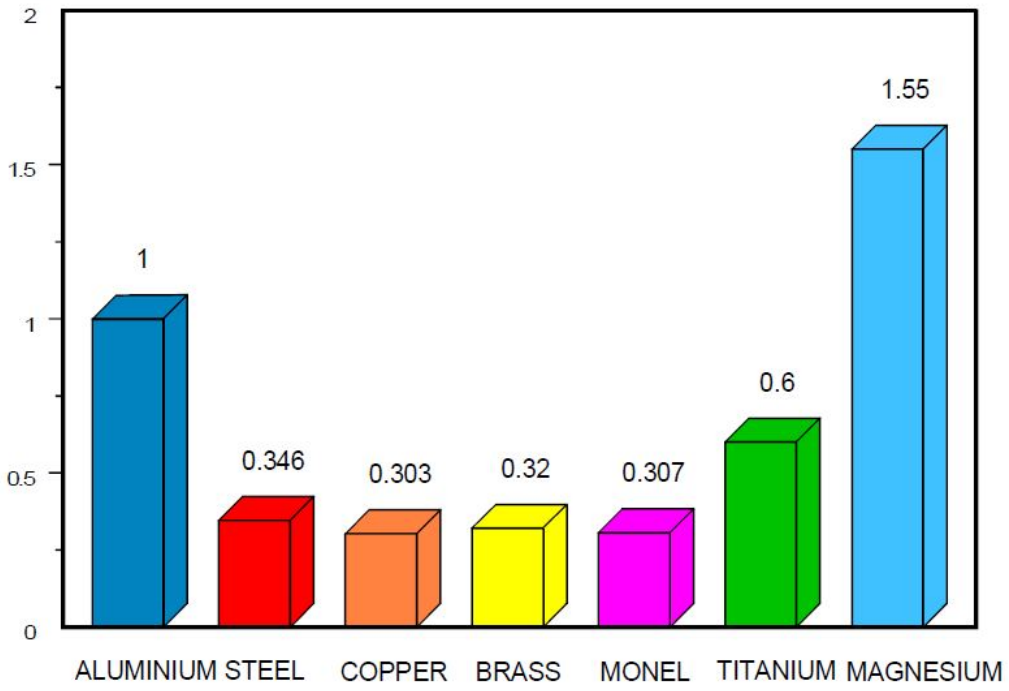

Figure 2: Volume per unit weight of common metals [1]

according to its lattice structure after changing state from the molten to solid state the crystalline structure stays the same more likely to copper, silver and gold FCC arrangement of atoms in its lattice structure. Having the atomic weight of 26.98 and specific gravity of 2.7 (nearly one-third of common metals) has turns lightness as a most fascinating characteristic of aluminum. The low density weight ratio with high strength possible has forced engineers to select aluminum as the most used material for aerospace industries over past sixty years [11].

Due to its low specific gravity and having the 63.8% of electrical conductivity in 99.99% of pure aluminum, the mass electrical conductivity is a way twice of annealed copper. The resistivity and conductivity are two sensitive properties that changes with chemical composition and the thermal treatment of alloy. This silvery metal is familiar to every household in the form of pots and pans, beverage cans, and aluminum foil. It is attractive, nontoxic, corrosion-resistant, nonmagnetic, and easy to form, cast, or machine into a variety of shapes. It has a melting point of 660 °C

and a boiling point of 2,519 °C.

Pure aluminum is relatively soft but not the strongest among metals. When melted together with other elements such as copper, manganese, silicon, magnesium, and zinc, however, it forms alloys with a wide range of useful properties [13]. Aluminum alloys are used in airplanes, highway signs, bridges, storage tanks, and buildings. The world's tallest buildings, the World Trade Center towers in New York, are covered with aluminum. Aluminum is being used so often in aerospace and automobile industries because it is only one-third as heavy as steel and therefore decreases fuel consumption [13].

2.1.3 Elevated Temperature Properties of Aluminum Alloys

7075 aluminum alloy, a high strength Al-Zn-Mg-Cu alloy, having noticeable room temperature strength to its density ratio, fracture toughness and corrosion resistance (specifically in T651 temper, has a typical tensile strength of 572 MPa, which is higher than many mild steels) has been widely used in automobile and aerospace industries, weapons and transportation fields as high-strength structural parts [14, 15]. Since usually these parts are formed by using as extruded bars, the microstructure should be sensitively controlled during hot deformation process to ensure the comprehensive properties of the parts [16].

Generally, in hot deformation of structural alloys as temperature rises the strength of alloys decreases, meanwhile with respect to processing conditions some other important mechanical properties such as toughness and ductility increases or even might decrease in unpredictable levels [17]. Basically, when discussing ductility of a material, both work hardenability and strain-rate sensitivity should be delicately controlled. The ability of a metallic alloy to be work hardened, which is mostly because of the interaction of microstructural defects such as dislocations and second phase particles within the lattice, is related to the deformation temperature. These would assign a

uniform region in plastic deformation of the stress-strain curves [18].

There have been several studies concentrating on the elevated temperate mechanical behavior of aluminum alloys. Tajally et al. [19] investigated the comparative tensile and impact-toughness behavior between cold-worked and annealed 7075 aluminum alloy. Panigrahi and Jayaganthan [20]. investigated the effect of aging on microstructure and mechanical properties of bulk, cryorolled and cold-worked Al 7075 alloy. Rokni et al. [21] investigated the hot compression deformation behaviors and microstructural evolution of 7075-T6 aluminum alloy. Jimenez et al. [22] characterized the superplasticity of severely deformed Al 7075 alloy by equal channel angular pressing at intermediate temperatures and observed the loss of superplastic behavior at temperatures above 350 °C which is reported due to abnormal grain growth and change of deformation mechanism.

As part of a study of grain orientation changes during hot deformation of Al alloys, a new method has been developed by Quey et al. [23] to characterize the evolution of deformation substructures and textures on the grains during plastic straining. This microtexture tracking method consists of the repeated cycles of deformation of a split sample with detailed EBSD texture maps of the area at various strains. They reported that the substructure maps of grains on a surface indicates that their dislocation substructure increases to a strain of about 0.5 then stabilises at approximately constant size, disorientation distribution and boundary alignment. The results are consistent with the model of steady state sub-boundary creation and dissolution during hot deformation [23].

Zhang et al. [24] conducted hot compression tests on 2026 aluminum alloy in temperature range of $300 - 450$ °C and strain rate range of $0.01 - 10$ s^{-1}. The correlation between compression conditions and microstructural evolution after solution and aging heat treatment was investigated. They found that the recrystallization and precipitation-hardening decrease at linear-decreasing regime and become stronger

at elevated temperatures and lower strain rates. These have a reverse-proportional behavior to the Zener–Hollomon parameter (Z) during hot deformation. For low Z parameter, fine recrystallized grains are rarely formed while the well-formed subgrains with clean high-angle boundaries and coarse precipitates seem to remain during heat treatment. For high Z parameter, a large number of fine equiaxed recrystallized grains are produced, and a high dislocation density with poorly developed cellularity and considerable fine dynamic precipitates are replaced by the well-formed subgrains and relatively coarse precipitates after heat treatment. They also reported that the average grain size after heat treatment decreases with increasing Z value. It was noticed that a mathematical relation between the average grain size and the Z value is obtained [24].

Jin et al. [25] reported the result of the hot compression tests of 7150 Al alloy that the peak stress level decreased with increasing deformation temperature and decreasing strain rate, which can be represented by a Zener-Hollomon parameter in the hyperbolic-sine equation with the hot deformation activation energy. In the deformed structures the elongated grains appear with serrations developed in the grain boundaries. Decreasing of Z value leads to more adequate proceeding of dynamic recrystallization and coarser recrystallized grains. The subgrains exhibit high-angle sub-boundaries with a certain amount of dislocations and large numbers of dynamic precipitates in subgrain interiors as increasing Z value. The dynamic recovery and recrystallization are the main reasons for the flow softening at low Z value, but the dynamic precipitates and successive dynamic particles coarsening have been assumed to be responsible for the flow softening at high Z value [25].

The influence of cooling rate after homogenization on the flow behavior of aluminum alloy 7050 was investigated by Lin et al. [26] over a range of temperatures, $300 - 450$ °C, with strain rates of $0.001 - 1$ s^{-1}. It was found that water-quenched alloy exhibited higher flow stresses than furnace-cooled alloy, and the difference in

the peak stress decreased with temperature increasing. The strain-hardening rate during the initial stage of hot deformation was higher for water-quenched alloy than furnace-cooled alloy. During deformation at low temperatures with the lowest strain rate, flow softening was observed for both alloys, but this effect was more significant for the water-quenched alloy. The activation energy of the water-quenched alloy was more than twice higher than that of the furnace-cooled alloy. With strain increasing, the activation energy decreased for both alloys. These phenomena were explained based on dynamic precipitation and coarsening during hot deformation according to microstructure examination.

An attempt to study the flow stress features of 2519A aluminum alloy was done by Li et al. [27] in the temperature range from 300 to 450 with strain rates of $0.01-10\ s^{-1}$. The results show that the deformation temperature and the strain rate have obvious effects on the flow characteristic, and the flow stress increases with increasing strain rate and decreasing temperature. The flow stress of 2519A aluminum alloy deformed in the strain rate range of $0.01-1\ s^{-1}$ shows a dynamic recovery character; while that deformed at the strain rates of $10\ s^{-1}$ and in the deformation temperature range of $350-450\ ^{\circ}C$ shows part dynamic recrystallization character. The processing map at the strain of 0.5 is obtained and exhibits two safe deformation domains ($350-400\ ^{\circ}C$ at $0.001\ s^{-1}$ and $300-450\ ^{\circ}C$ at $1-10\ s^{-1}$). According to the processing map and microstructure observation, the optimum hot-working condition for 2519A aluminum alloy is determined to be $450\ ^{\circ}C$ and $10\ s^{-1}$ [27].

Spigarelli et al. [28] investigated the high-temperature plasticity of an AA6082 aluminum alloy in a wide range of temperatures and strain rates by means of torsion tests. The strain-rate dependence on stress and temperature was described by means of a modified form of the sinh equation, where the peak flow stress was substituted by the effective stress, i.e. by the difference between peak stress and a threshold stress, representing the strengthening effect of the particles. This analysis confirmed earlier

speculations that the high values of apparent activation energy frequently observed for heat-treatable alloys were related to the presence of precipitates, and quantified this strengthening effect.

The dynamic and static softening behaviors during multistage hot deformation of aluminum alloys (1050, 5182 and 7075 alloys) was studied by Hang et al. [29] in 300 and 400 °C at a strain rate of 0.5 s^{-1}. The interrupted deformations were conducted with delay times varying between 30 and 120 s after achieving a strain of approximately 0.4 in the first stage. It was indicated that the considerable dynamic softening and exceptional softening associated with a structure softening exist in both 1050 and 7075 alloy deformation at 400 °C, leading to an initial flow stress value at the second deformation lower than that at the first deformation. For all alloys studied, the static softening increases with increasing deformation temperature and holding temperature and delay times, but the increment for 5182 alloy is much higher than that for both 1050 and 7075 alloys in the same hot deformation conditions.

The hot deformation behavior of porous FVS0812 aluminum alloy prepared by spray deposition was studied by means of compression tests conducted by Zhan et al. [30]. The samples were hot compressed at temperatures ranging from 573 K to 773 K under various true strain rates of $10^{-4} - 10^{0}$ s^{-1}. The deformation behaviors are characterized by a significant strain hardening during hot-compression due to the progressive compaction of the pores with increasing compressive strain. A revised formula describing the relationships of the flow stress, strain rate and temperature of the porous alloy at elevated temperatures is proposed by compensation of strain. The theoretical predictions are compared with experimental results, which show good agreement [30].

The metadynamic recrystallization behaviors in deformed 2124 aluminum alloy were investigated by isothermal interrupted hot compressive tests, which were carried out at the deformation temperatures of (653-743) K, strain rates of (0.01-10) s^{-1}

and inter-stage delay time of (30-180) s [31]. A new approach, "peak stress method", is proposed to calculate the softening fractions induced by the rapid metadynamic recrystallization. The kinetic equations were developed to predict the metadynamic recrystallization behaviors in hot compressed 2124 aluminum alloy. Both the experimental and predicted results show that the effects of deformation parameters, including strain rate, deformation degree and temperature, on the softening behaviors in the two-pass hot compressed 2124 aluminum alloy are significant. A good consistency between the experimental and predicted results indicates that the proposed kinetic equations can precisely estimate the softening behaviors and metadynamic recrystallization kinetics of the hot compressed 2124 aluminum alloy [31].

An attempt to deform AA 3104 aluminum alloy was done by Liu et al. [32] to deform the material at temperature of 510 °C and at a strain rate of 5 s^{-1} to strains of 0.14, 0.53, 1.52, and 2.49 by plane strain compression. The effect of grain orientation on microstructures has been investigated using transmission electron microscopy (TEM). The results show that the grain orientation has a strong effect on the microstructures at low strains.

The microstructures can be classified into three types according to the process of grain subdivision and the characteristics of dislocation boundaries. Every type of microstructure is concentrated in a positive district in orientation distribution figure. The microstructures in grains near the brass and S orientations correspond to the Type AI microstructure. The grains near the copper orientation appear as a Type AII microstructure. The Type B microstructure is found in the region near the rotated Goss orientation. The Type C microstructure is concentrated in the cube orientation. At large strains approximately equiaxed subgrains are observed.

According to the experimental results, some constitutive models are proposed to delicately monitor the hot deformation behavior of metals or alloys; Peng et al. [33] has proposed an improved Arrhenius type model to describe the tensile behavior of CP-Ti

by considering the competing process of deformation mechanism. Khamei et al. [34] investigated a constitutive equations to developed the model of hot ductility of the severely plastic deformed AA6061 alloy. Sajadifar and Yapici [35] has predicted the workability characteristics and the flow behavior of severely deformed pure titanium by using Arrhenius type and dislocation density based models [36].

Xizhou et al. [37] proposed the constitutive modeling and processing map to obtain the rheological properties of the 6X82 aluminum alloy at different temperatures and strain rates. Saravanan and Senthilvelan [38] reported the hot deformation behavior analysis and processing map for the fabrication of Al7075-Al2O3 nanocomposite using a three-step mixing cum stir-casting method. Eivani and Karimi [39] used a beneficial equation to estimate the hardness of an Al-Mg-Si-Cu alloy with a remarkably good agreement. To the knowledge of the authors, there is not such a simple and precise model to evaluate the effect of age hardening on the hardness of the alloy. El Mehtedi and et al [40] introduced a revised form of the HS equation (developed by Hensel and Spittel) to describe the hot workability of an AA6083 aluminum alloy.

As a common fact of all reviewed researches above, it can be concluded that the hot ductility and deformation behavior of Al-Zn-Mg-Cu alloy is significantly influenced by its grain size, strain rate, second phase particles of the grain boundaries, deformation mode and so on. Despite remarkable researches invested into hot deformation characterization of Al-Zn-Mg-Cu alloys, adding a comparative high temperature deformation behavior between O-tempered and severely rolled conditions, in addition to failure characteristics investigation in order to provide an optimum forming processing conditions of Al 7075, could perfectly fill this gap.

2.1.4 Heat-Treatable and Non-Heat-Treatable Alloys

Alloys that can be thermal treated, according to their phase solubility are considered as solution heat treatment process which is mainly followed by water quenching

and later naturally age hardening and artificial age hardening. Whether they are cast or wrought, they are referred to as heat treatable. Heat-treatable aluminum alloys usually contain magnesium, plus one or more other alloying elements such as copper, silicon and zinc. In the presence of those elements, even small amounts of magnesium promote precipitation hardening. These alloys respond to heat treatment because their key alloying elements show increasing solid solubility in aluminum with increasing temperature in which this raise of strength induced by heat treatment can be dramatic [14].

Most of wrought aluminum alloys are mainly processed through work hardening by mechanical reduction, as well as some casting alloys, are not as heat treatable; they usually appear to be non-brittle metals with a reasonably high melting point. Alloys not prone to heat treatment are referred to as non-heat-treatable [15, 16]. Strain-hardened alloys containing appreciable amounts of magnesium are usually given a final elevated temperature treatment to stabilize their properties. Cold-working can increase strength significantly in non-heat-treatable alloys. Both heat-treatable and non-heat treatable alloys may be deliberately softened and made more formable by annealing [14].

Heat treating process of aluminum alloys consists of controlled cycles of heating and cooling in which normally by increasing the strength of alloy in that specific heat treatment, the formability may sometimes be affected. Usually alloys in the 2000, 6000 and 7000 series are heat treatable while, non-heat-treatable aluminum alloys are hardened by strain hardening without heat treatments. Moreover, aluminum alloys in the 1000, 3000, 4000 and 5000 series are strengthened by work hardening [15–18].

The 3000 series is mostly used in cooking utensils and chemical equipment, due to its superiority in handling many foods and chemicals; the AA3104 or 3004 in particular is the largest volume alloy combination in the industry, with applications in the bodies of beverage cans. The 5000 alloys have wide applications in the top of

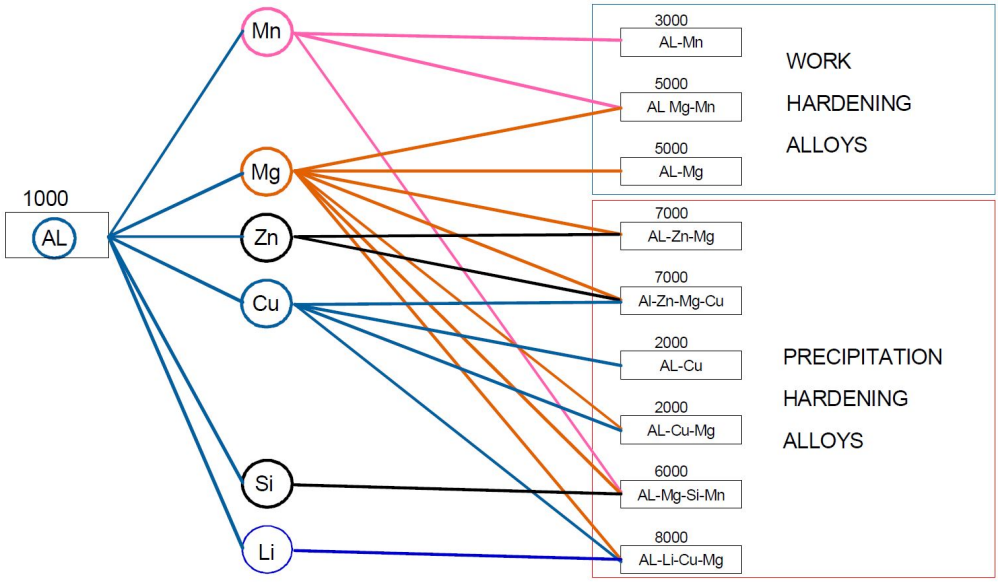

Figure 3: Main alloy types available as sheet and plate [1]

the beverage can, automotive, building and construction areas [16–19].

The aluminum alloy compositions are registered with the Aluminum Association (AA). The 3000 and 5000 series are alloyed with manganese and magnesium respectively. Both of these additions increase strength primarily by solid solution hardening and by forming precipitates such as S (Al_2CuMg), η ($MgZn_2$) and Al_3Mg_2 which could control recrystallized grain size by pinning grain and sub-grain boundaries [41]. At the eutectic temperature, the limit of manganese solubility is 1.5 wt% and magnesium solubility is 17.4 wt% in aluminum [20]. The present system utilized to identify wrought aluminum alloys is the four digit designation system, shown below:

- The 1000 series are essentially pure aluminum with a minimum 99% aluminum content by weight and can be work hardened.

- The 2000 series are alloyed with copper and can be precipitation hardened to strengths comparable to steel. Formerly referred to as duralumin, they were once the most common aerospace alloys, but were susceptible to stress corrosion cracking. They are increasingly replaced by 7000 series in new designs.

- The 3000 series are alloyed with manganese, and can be work hardened.
- The 4000 series are alloyed with silicon. They are also known as silumin and are heat treatable.
- The 5000 series are alloyed with magnesium and can be work hardened.
- The 6000 series are alloyed with magnesium and silicon, are easy to machine, and can be precipitation hardened, but not to the high strengths that 2000 and 7000 can reach.
- The 7000 series are alloyed with zinc, and can be precipitation hardened to the highest strengths of any aluminum alloy.
- The 8000 series is a category mainly used for lithium alloys, heat treatable.
- The 9000 series is reserved for future use.

The work hardening rates can be different for different alloy series, for instance, AA3104, AA5182 and AA9111 have high work hardening rates at low temperatures and the work hardening amount decreases while temperature increases, due to dynamic recovery. The compositions and grain sizes between different series are different. Even in the same series, the composition can be very different.

All aluminum alloys can be rolled to sheet but, with a few notable exceptions mentioned below, the ones utilized are from the 1000, 3000 and 5000 series which are work hardening alloys. However, the 2000, 7000 and 8000 heat treatable alloys are used for airframes, 2000 and 6000 series for automobiles and the 6000 series for some pressure vessels and containers. Examples exist for the use of plate in all alloys while foil is almost all from the 1000 series.

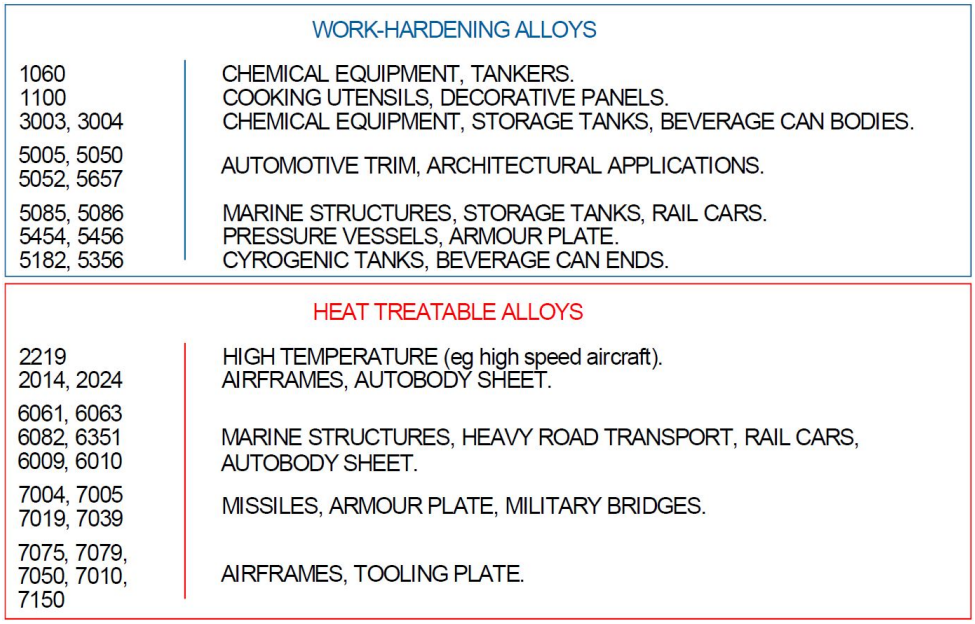

Figure 4: Typical applications of some aluminum sheet and plate alloys [1]

2.2 Heat Treatment of Aluminum Alloys

2.2.1 Purposes of Annealing

Aluminum alloys may be hardened by hot or cold rolling procedures to a degree that is not desired in the finished product or that would interfere with further rolling and the achievement of a desired temper. Heat-treatable alloys may be sufficiently heated and cooled during hot-rolling to undergo some partial solution heat treatment and precipitation hardening [21].

Cold rolling, on the other hand, elongates grains and sets up internal stresses and strains. These changes create resistance to further deformation in cold-rolled plate or sheet is said to become work-hardened. Unwanted precipitation hardening or work hardening is removed before further rolling or product finishing by annealing that is, by heating the aluminum alloy above its recrystallization temperature and holding it there long enough for the grain structures created earlier to re-crystallize and relieve the internal stresses. Annealing can be applied at any stage in the rolling process [21, 33].

2.2.2 Full Annealing

Recrystallization temperature is not a precise term and it does not occur suddenly at a sharply defined temperature; instead, it begins gradually as the temperature rises into an effective range, and it progresses to completion over an extended time. The effective recrystallization temperature depends on the deformation and thermal treatment conditions it has previously undergone, as well as the annealing soak time [42].

Full annealing converts both heat-treatable and non-heat-treatable wrought alloys into their softest, most ductile, most workable condition, designated as the O-temper. For full annealing of heat treatable wrought aluminum alloys, the metal is typically soaked for about two hours at a temperature in the range of $335 - 370$ °C to remove cold work, or $400 - 425$ °C to counteract heat treatment [43]. Then the metal is cooled slowly, at a closely controlled rate appropriate to the alloy. This permits maximum coalescence of precipitating particles, minimizing hardness.

Non-heat-treatable alloys are annealed by heating for one-half hour to two hours (most often about one hour) at a temperature in the range of $335 - 405$ °C. Then they are cooled at a controlled rate [43]. Annealing also provides the conditions for stress-relief and may even be applied specifically for that purpose if furnace schedules and product requirements permit.

The H1 and H3 aluminum alloy tempers are created by applying specific amounts of strain hardening to fully-annealed metal. These are called rolled-to-temper products. Cold rolling prior to roll bonding inflicts the material with high stresses that gives high strength, but may also decrease the ductility severely. To eliminate some or all of the effects of this work hardening, a heat treatment called annealing may be performed. However, the strength gained by cold rolling will decrease during this process as well [43].

There are two main softening reactions occurring when a heavily deformed material is fully annealed, and these are called recovery and recrystallization [34]. Before explaining these two phenomena in more detail, let it be said that recovery and recrystallization is competing processes driven by the same stored energy, created by the deformation. Once the stored energy has been consumed by one or the other, no further recovery or recrystallization can occur. Hence they are strongly dependent on each other [33].

2.2.3 Dynamic Recrystallization

One of the principal metallurgical phenomena in cold to hot deformation of metals is dynamic recrystallization (DRX), owing to formation of new grain structure in plastic deformation of the fine grain materials. These newly formed fine grains during the DRX can be obtained under relatively warm deformation, i.e. $T \leq 0.5\ T_m$ where T_m is the melting point.

Creation of new fine grains during cold to warm deformation is dependent on the rate of straining and temperature, often occurs in alloys with high stacking fault energy (SFE) during the hot deformation, i.e. aluminum alloys [22]. It is worth noting that this softening mechanism is an impressive method to refine the coarse grain and reduce the hot deformation resistance. Consequently, the mechanical behaviors of alloys can be improved. There have been many studies discussing the structural mechanism for evolution of new fine grains during DRX [22, 23, 35].

2.2.4 Dynamic Recovery

Dynamic recovery (DRV) is known as a prevailing softening mechanism regime in hot deformation by which deformed grains can reduce their stored energy by the removal or rearrangement of defects, primarily dislocations, in their crystal structure. This rearrangement is the result of sliding of dislocations out of their slip plane [24]. This process is known as the most common softening mechanism in metals with high stacking fault energy, e.g. aluminum, alpha-Fe, and most BCC metals where climb and cross slip of the dislocations are relatively easy [25].

The active dislocation movements within hot working are both screw and edge dislocations that can leave slip planes to substitute with opposite side and annihilate. These process can be accelerated not just by elevated temperature but also by stresses and high vacancy concentrations which are present in the metal during plastic deformation [24]. Accordingly, the mis-orientation of sub-boundaries is maintained sufficiently low such that they never become capable of moving as grain boundaries of recrystallization nuclei. Deformation at constant temperature and strain rate is necessary to appoint stress-strain curve. Specifically for aluminum alloys, the flow curves usually exhibit monotonic hardening to a steady-state plateau level of stress.

The Al alloy strain hardens monotonically to a steady state as a result of DRV which is high at 400 °C but low at 200 °C as illustrated by substructure diagrams (Fig. 5). Moreover, if the material is given a low-temperature heat treatment, the additional energy allows the dislocations to move and form new boundaries. This new formation is called a polygonized sub-grain structure. The term for this stage is recovery and refers to the changes in a deformed material which partially restore the properties to its pre-deformed state [24].

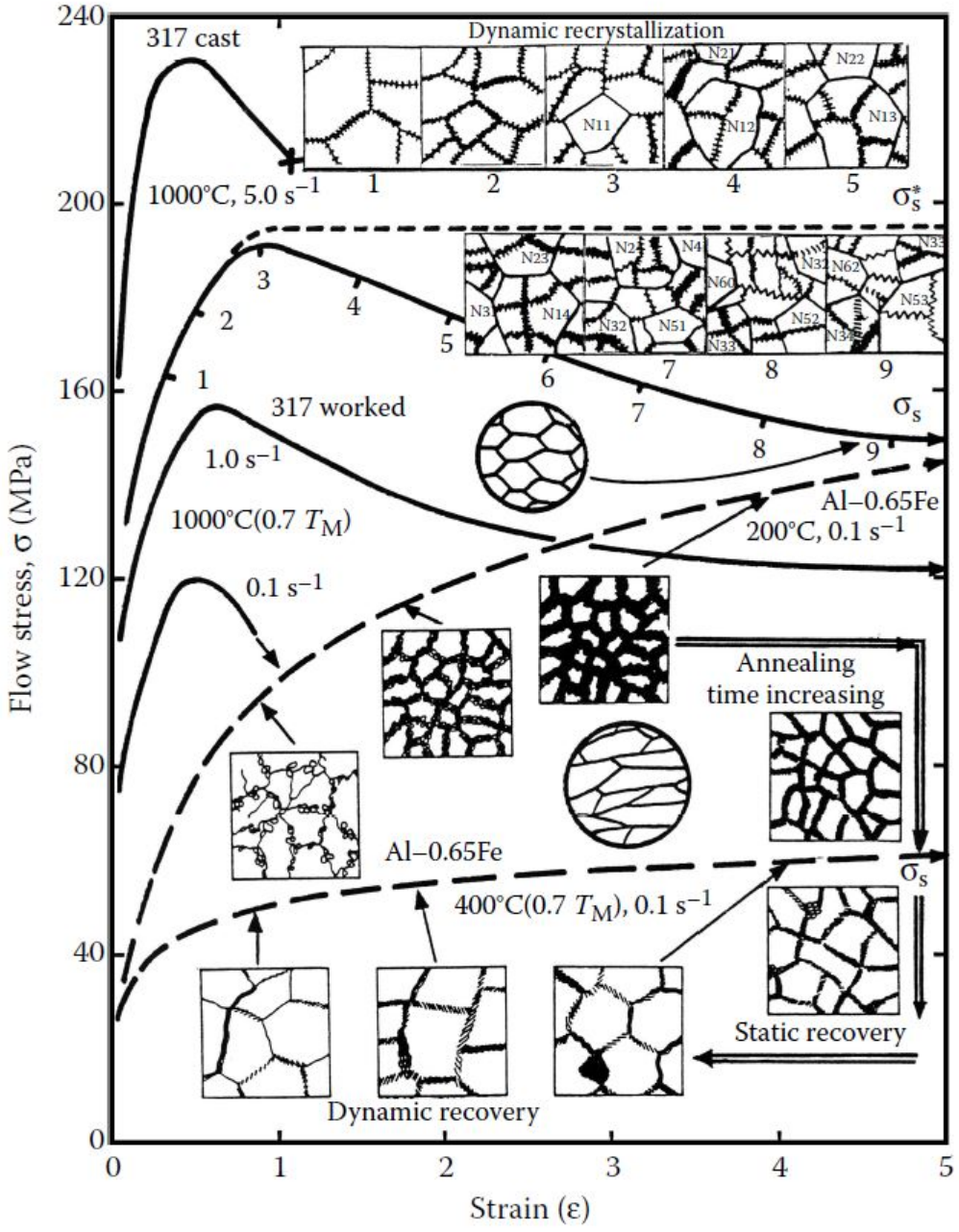

Figure 5: Torsional stress-strain curves for Al-0.65Fe and 317 stainless steel at about 0.7 T_m [2]

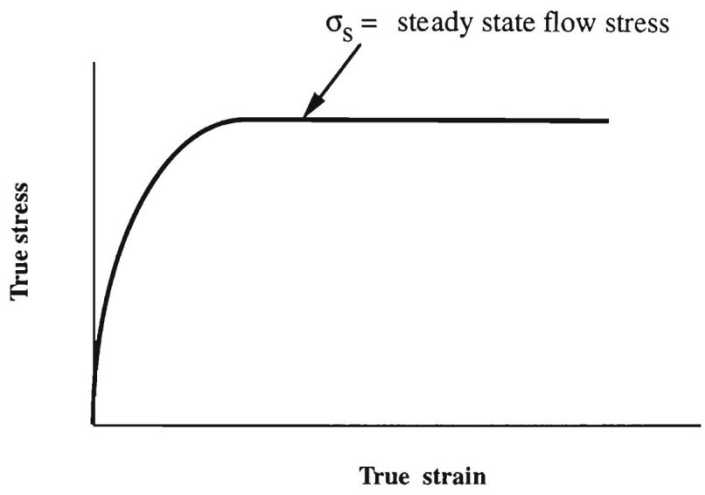

Figure 6: Schematic flow curve for a metal that shows dynamic recovery during hot working [2]

Residual stresses due to work hardening are removed, although no change in dislocation density occurs. At this temperature the mechanical properties is relatively unchanged. A schematic (Fig. 6) shows the steady-state uniform region, due to dynamic recovery [2].

CHAPTER III

DESIGN AND EXPERIMENTAL PROCEDURE

3.1 Material

The material used for this investigation was a commercial aluminum alloy 7075-T651 which has been supplied by Vimetco Alro, Romania, with chemical compositions given in Table 1. The as-extruded plate of Al 7075-T651 has machined along the extrusion direction to the rectangular billet of $80mm \times 50mm \times 10mm$ (Fig. 7).

3.2 Annealing

Full annealing heats the alloy hot enough, long enough, to soften the product completely that is, to achieve full recrystallization [14]. During the aging process of T651 temper, GP (Guinier-Prestone) zone and a small fraction of η' phase is being formed in the microstructure of 7075. The formation of the η' phase indicates over-aging and results in decreased strength properties [26]. To decrease the effect of residual stresses in material and avoid possible failure in cold-work, plus to reach higher reductions in cold rolling process by softening the material, it is important to fully anneal the as-received T651. Fig. 8 shows the rolling failure of a T651 slab after applying the cold work.

Table 1: Chemical composition of the studied aluminum alloy

Elements	Zn	Mg	Cu	Cr	Fe	Si	Ti	Mn	Al
Wt%	5.5	2.27	1.37	0.21	0.2	0.097	0.033	0.02	Balance

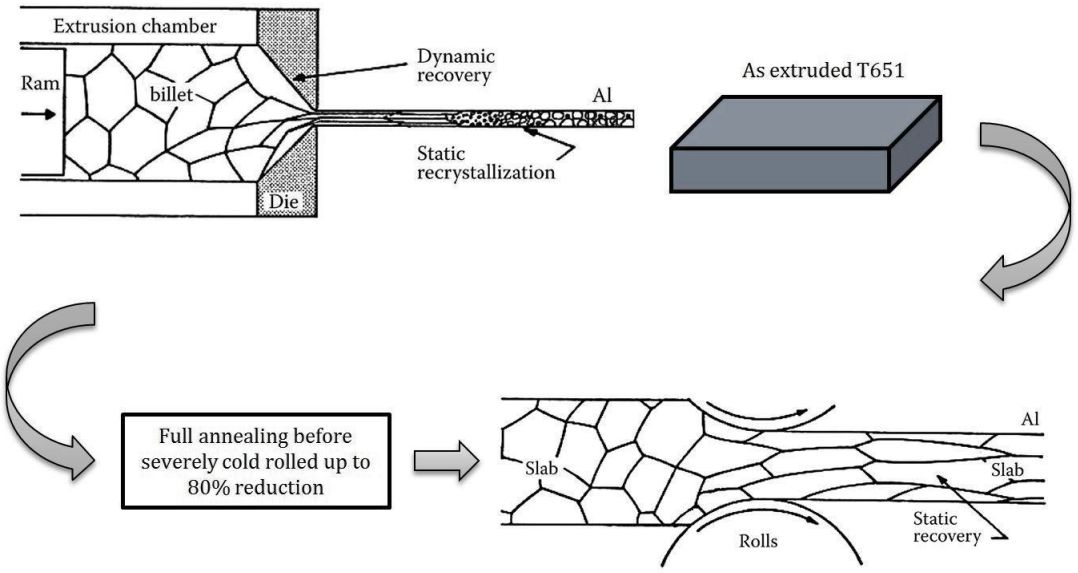

Figure 7: Mechanical process of annealing and cold rolling on the as received T651 aluminum alloy

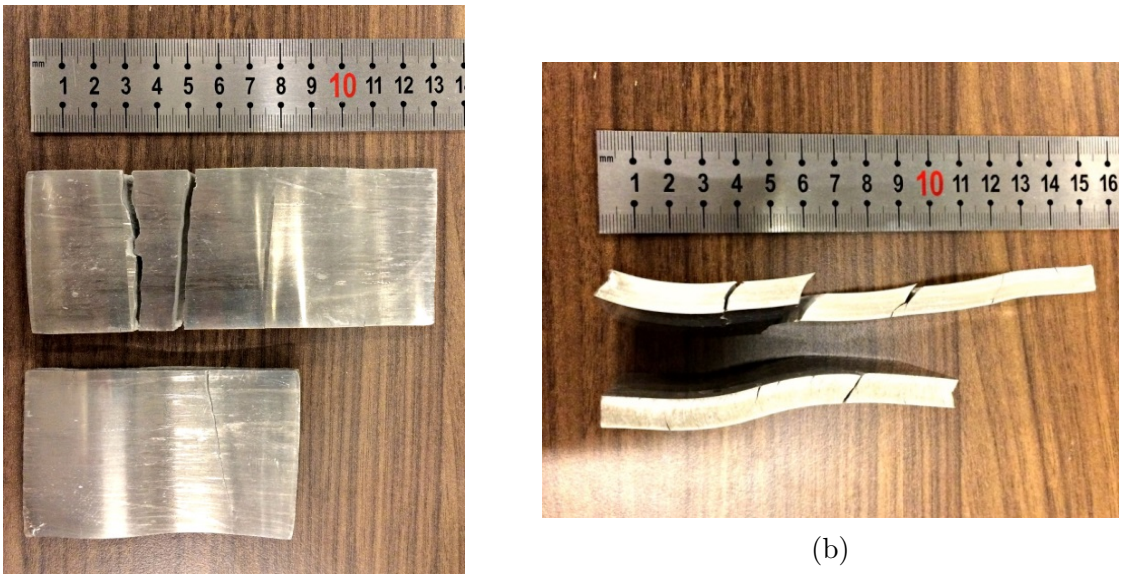

(a) (b)

Figure 8: Cold rolling failure of T651 condition

Figure 9: Bilets in annealing furnaces

Annealing (O-temper condition) of the billet was performed at 420 °C for 180 min followed by furnace cooling that allows maximum coalescence of precipitating particles as minimizing hardness (Fig. 9). Empirical experiences have determined that furnace cooling followed by annealing process, is facilitating the rolling process in comparison to other techniques of quenching [27].

Cold rolling of annealed billets was carried out by using of roll mill machine at room temperature (Fig. 10). The thickness reduction took place from 10.3 mm down to 2.3 mm ($80 \pm 2\%$) with a constant and equal amount of reduction in each pass for all the billets. Since the amount of deviation from the rolling direction was negligible for all the billets that cold working has applied to them, the effect of anisotropy on mechanical properties of rolling sheets could not be the matter of discussion. Moreover, with respect to the fact that the maximum tensile strength could only be achieved in the direction of rolling, all the specimens have been prepared in the rolling direction.

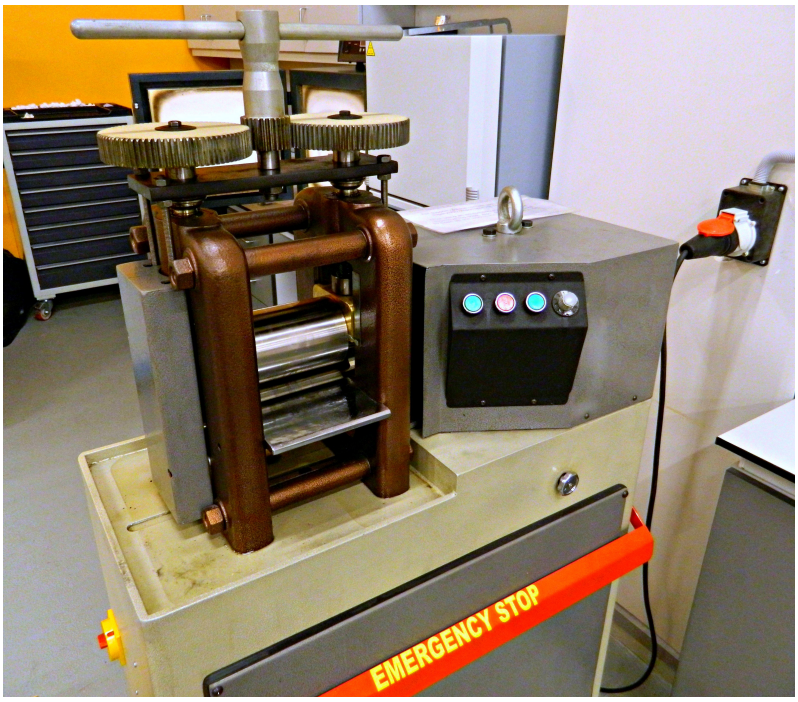

Figure 10: Roll mill machine

3.3 Mechanical Characterization

Tensile tests were accomplished employing a delicate computer-controlled servo-hydraulic Instron machine equipped with an intermediate-temperature sliding chamber. The high temperature test set up was designed and calibrated according to the repetitive tensile tests (Fig. 11-14) The heat sources inside of the chamber were supplied by two band heaters. Although the generated heat in chamber assigned to control by two precise controllers, but to have a delicate control of heat surrounding the specimen we externally attached a K-type thermocouple right on the surface of the specimen during all performed hot tensile tests.

The tests were conducted at room temperature, 200, 250, 300 and 350 °C in various crosshead speeds of 0.1, 0.01 and 0.001 s^{-1} where data capturing of tensile deformation performed by a hot mountable furnace extensometer. The temperature range corresponds to $0.5 - 0.66$ T_m, where T_m is the absolute melting point of the Al7075 alloy. The tensile tests specimens were machined by CNC EDM wire-cut from

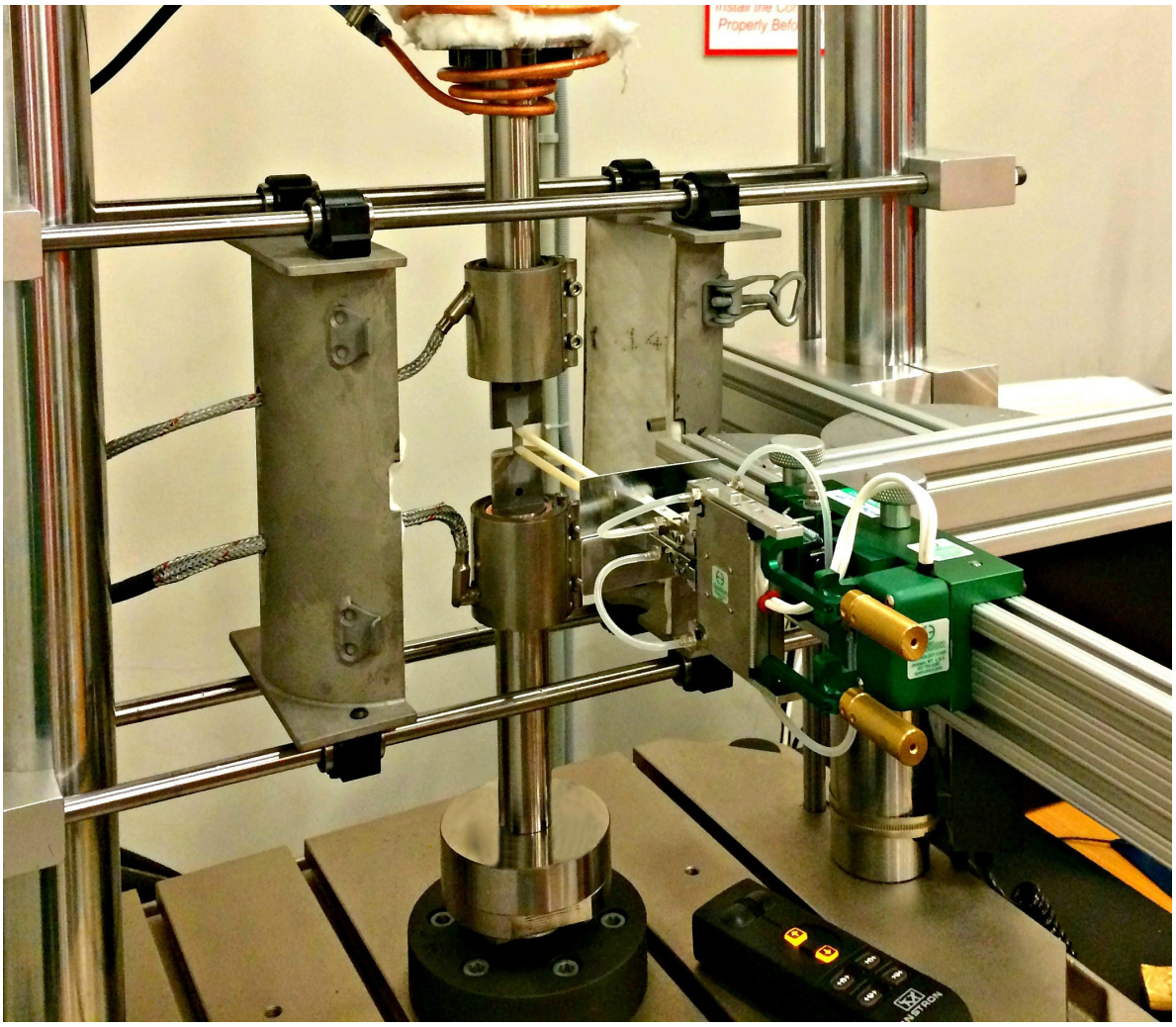

Figure 11: High temperature test set up

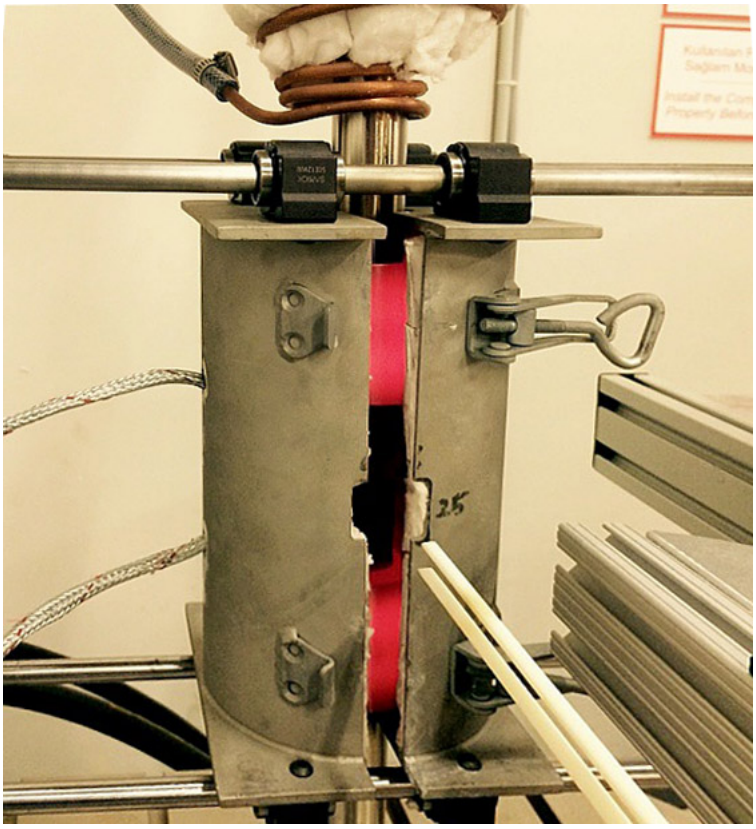

Figure 12: Sliding isolated high temperature chamber

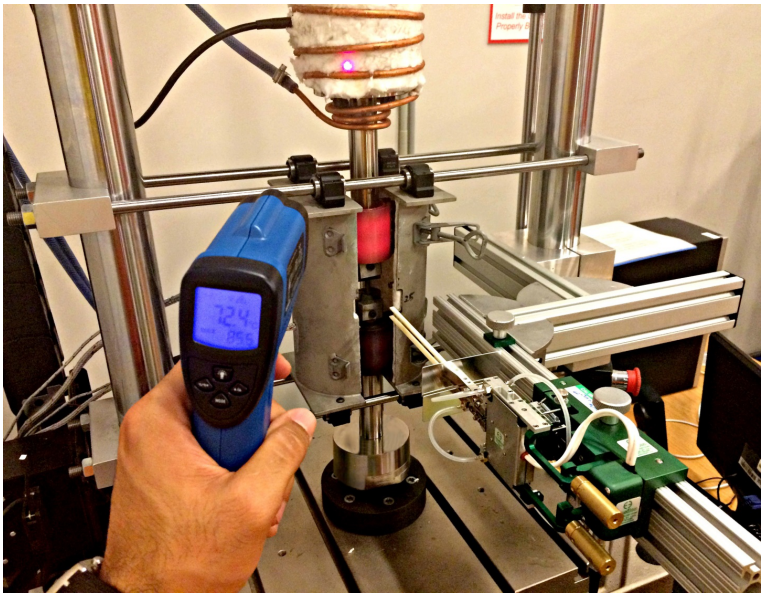

Figure 13: Checking the heat loss by a laser gun while sliding chamber is opened to avoid possible damages

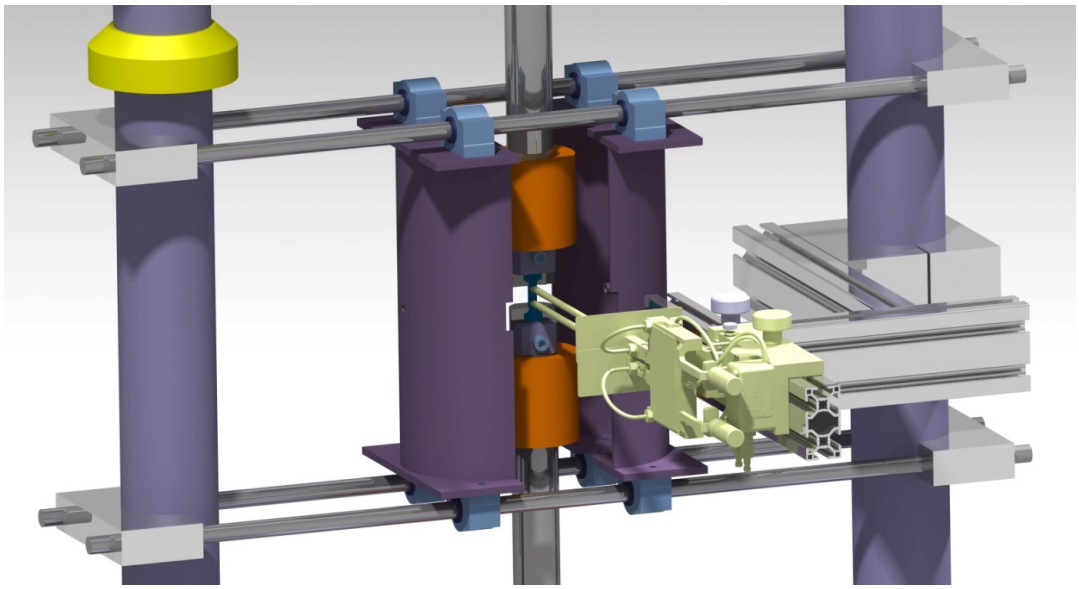

Figure 14: The 3D model of hot tensile test setup

both annealed and rolled billets of Al 7075 along the extrusion and rolling direction with the gage length of 15 mm. The elevated temperature tensile tests were carried out in uniformly constant temperature chamber. Prior to loading, the specimens were heated and kept in the desired deformation temperature at a heating rate of 25 $^{\circ}C/min$ and held isothermally for 10 min to obliterate thermal gradient. Later on, the specimens were loaded under demanded strain rate and temperature. This was followed by quenching the fractured specimens in water right after straining.

3.4 Metallographic Characterization

Metallographic samples were prepared by sectioning all the conditions by use of cut-off wheel machine so as to prepare them for metallography on the rolling plane. The metallographic specimens were prepared by mounting the specimens in to different dies to be able to polish them via grinding. Polishing was carried out by use of diamond suspension (< 1 μm) and alumina nanopowder (< 50 nm). The polished metallographic specimens were anodized by using Barker's reagent (5 ml HBF4 (48%) in 200 ml water) at 30 V direct current (DC) according to ASTM standards

Figure 15: Optical macroscopic (OM) sample preparation for all tested conditions

(E407) for grain structure under polarized light. A ZEISS optical microscope, Axio Imager A2 model, equipped with transmitted polarized-light bright field, with ergo-tube 20°/23 linked with a computerized imaging system (software) was employed for metallography observations.

3.5 Fracture Surface Characterization

For characterizing the fracture surface of the aluminum samples, scanning electron microscopy (SEM) and also energy dispersive spectrometer (EDS) were utilized. The SEM study with a JEOL brand machine was completed at 20 kV with Secondary Electron Images (SEI).

CHAPTER IV

RESULTS AND DISCUSSION

4.1 Tensile Behavior of Studied Al-Zn-Mg-Cu Alloy

4.1.1 Ambient Temperature Tensile Deformation

Fig. 16 demonstrates the tensile stress-strain curves of both annealed and rolled samples at room temperature. It can be seen that cold rolling procedure is capable of increasing the strength of Al7075 alloy. Severe cold deformation as well as low deformation temperatures can generate high density of dislocations. Therefore, the strength of the processed materials can be enhanced. However, cold deformation reduced the ductility of this material. Ductility decreased with the increase of dislocation density due to the fact that dislocation movement remains low because of large number of dislocations and introduced defects [27].

Mean values for UTS (Ultimate Tensile Strength), YS (Yield Strength) and elongation to fracture of Al7075 alloy in different conditions are represented in Table 2 and 3. YS values of both annealed and rolled specimens considerably decrease with increase of deformation temperatures. It would mean that commence of plastic deformation of Al7075 alloy requires less stress at elevated temperature which can be attributed to activation of softening mechanisms [44]. The YS and UTS levels of rolled samples are remarkably higher than that of annealed samples at temperatures below 250 °C. However, strength levels of annealed specimens surpass the rolled ones at temperatures above 250 °C. This behavior can be due to acceleration of DRV and DRX phenomenon in rolled specimens. It is well-known that cold deformation procedure is able to increase the stored energy and the number of potential nuclei [45]. Therefore, temperature of onset recrystallization drops in the rolled specimen.

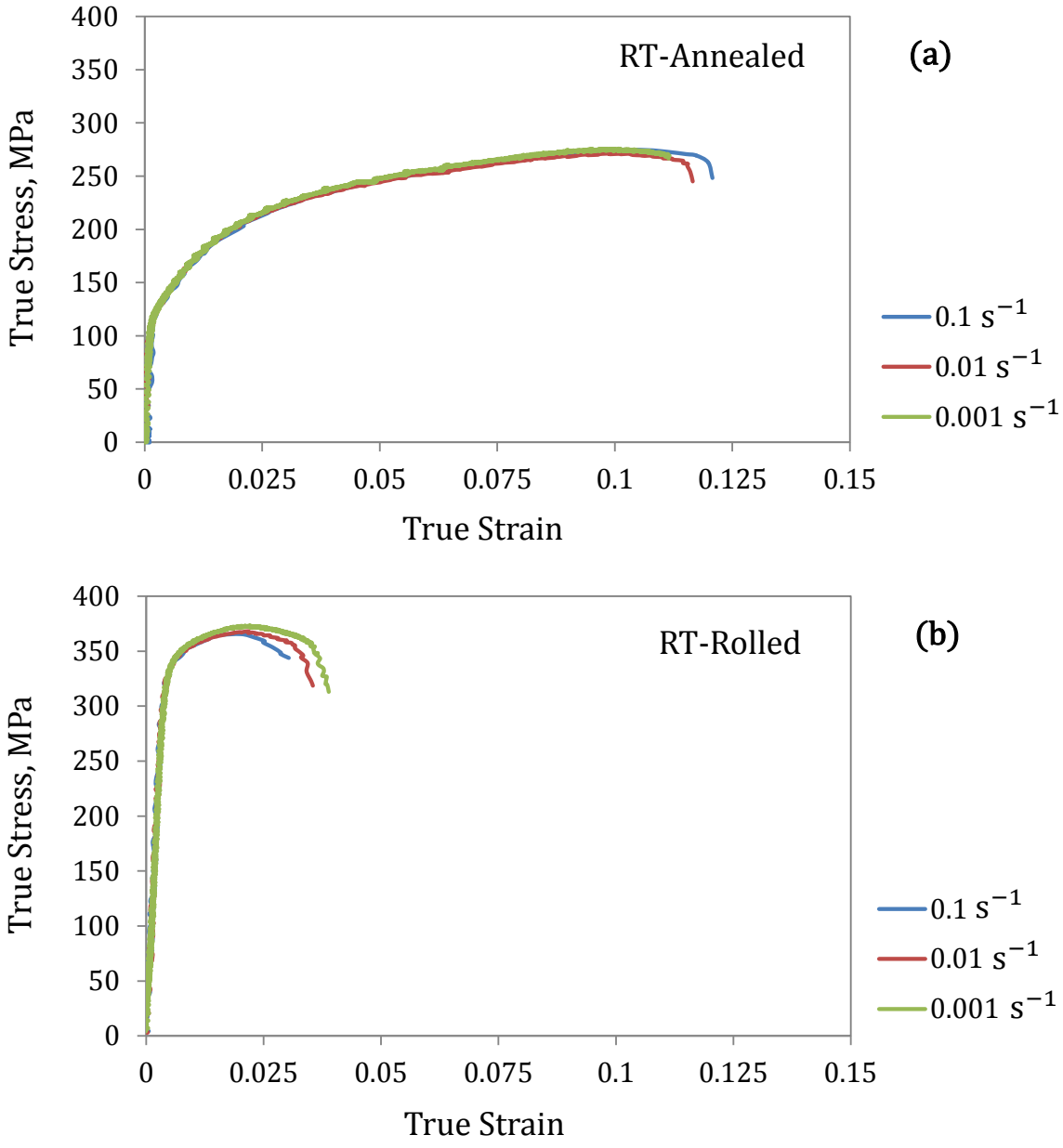

Figure 16: The ambient temperature tensile true stress-strain curves of (a) annealed (b) cold rolled Al 7075 alloy

Table 2: Mechanical properties of the annealed sample

Deformation	**Tensile Properties**			
Temperature	$\dot{\epsilon}(s^{-1})$	**Yield Strength (MPa)**	**UTS (MPa)**	**EL (%)**
Ambient	0.1	118	249	12.93
	0.01	120	246	12.76
	0.001	121	251	13.32
200°C	0.1	94	157	19.18
	0.01	90	132	18.74
	0.001	84	102	17.31
250°C	0.1	99	121	16.36
	0.01	81	94	15.4
	0.001	72	74	16.1
300°C	0.1	94	106	19.44
	0.01	72	84	17.33
	0.001	50	57.5	19
350°C	0.1	80	85	17.63
	0.01	68	73	17.95
	0.001	47	51	18

Table 3: Mechanical properties of the rolled sample

Deformation	**Tensile Properties**			
Temperature	$\dot{\epsilon}(s^{-1})$	**Yield Strength (MPa)**	**UTS (MPa)**	**EL (%)**
Ambient	0.1	234	359	4.15
	0.01	221	360	3.83
	0.001	174	366	3.96
200°C	0.1	125	218	22.47
	0.01	93	160	18.07
	0.001	44	111	26.5
250°C	0.1	99	163	33.85
	0.01	61	106	47.31
	0.001	40	71	47.2
300°C	0.1	75	104	22.62
	0.01	57	75	54.6
	0.001	50	51	48
350°C	0.1	76	89	32.68
	0.01	56	65	55.9
	0.001	45	49	37

The O-tempered 7075 Al alloy plates find industrial applications due to their higher formability in comparison to the other temper conditions. It was also observed that both cold rolled and annealed specimens were not sensitive to the rate of deformation in the range of 0.001 to $0.1s^{-1}$ at room temperature.

4.1.2 High Temperature Deformation Behavior

As an engineering method to analyze the plastic deformation behavior of materials, the true stress vs true strain curve for both annealed and rolled conditions are presented in Fig. 17 and Fig. 18. It is obvious that the flow stresses in an uniaxial tensile test are strongly affected by applied temperature and strain rate. Increasing the deformation temperature or decreasing the strain rate can result in the decrease of peak stress, as shown in Fig. 19.

The mentioned phenomenon can be attributed to the low strain rate providing longer time for energy accumulation and high deformation temperature enhancing the thermal activation process, which would accelerate the dislocation motion facilitating dynamic softening and as a result reducing the peak stresses [28]. It can be distinguished that the strain rate has complex effects on the deformation and fracture behavior of the severely rolled samples whereas in annealed condition this effect is not tangible. By increasing the strain rate, tangled dislocation structures act as an obstacle against the dislocation movements which would shrink the plastic deformation capability of samples. On the contrary, for the lower strain rate values, the microvoids or microcracks have enough time to grow and coalesce which would lead the material in failure with low amount of deformation. Thus, the variation of the elongation to fracture with strain rate is not monotonous [28]. Accordingly, the maximum elongation to fracture is usually reported under the strain rate of 0.01 s^{-1} and deformation temperature of 350 °C for the severely rolled condition. Fig. 18 demonstrates the true stress-true strain curves for the uniaxial tensile tests of the

rolled aluminum alloy Al7075 samples at various temperatures for the strain rates of 0.001, 0.01 and 0.1 s^{-1}.

Tensile tests were conducted on annealed and rolled conditions. The flow stress slightly rises to a peak and then decreases gradually and reaches a plateau at higher deformation temperatures. This behavior could be attributed to the obvious necking stage at elevated temperature which also was observed in previous literature [28]. It is worth noting that stress levels of rolled samples are higher than that of annealed ones at lower deformation temperatures.

This is related to the higher fraction of dislocations in rolled samples causing work hardening during hot deformation. In contrast, stress levels of rolled samples are lower than those of annealed ones especially at very high deformation temperatures. This behavior can be linked to occurrence of dynamic recovery (DRV) and dynamic recrystallization (DRX) at cold rolled samples. It is well-known that cold deformation can accelerate DRX and DRV, since it increases the dynamic force of softening mechanisms [29]. The steady state level is evident for annealed samples at all conditions although fracture takes place at lower strain values. Rolled specimens reached higher elongation levels which can be attributed to fine structure of this condition.

It is well-known that fine grains can lead to significant superplasticity levels since the dominant deformation mechanism in fine structure is grain boundary sliding (GBS) [30]. Moreover, higher ductility was observed in rolled samples at moderate strain rate of 0.01 s^{-1}, as well. Low levels of ductility at the low strain rate of 0.001 s^{-1} would be related to the void coalescence [28], whereas at higher strain rate of 0.1 s^{-1}, under relatively low temperature since the DRX is not the dominant active deformation mechanism, this behavior is not reported [46].

Fig. 19 summarizes the flow stress as a function of strain rate and temperature. It is worth mentioning that the peak flow stress of both annealed and rolled samples

depends strongly on the deformation temperature and strain rate. However, sensitivity of rolled samples to both deformation rate and temperature is much more obvious than annealed samples. Observance of this behavior can be due to occurrence of onset of DRX which can soften materials at elevated temperatures. It was reported that dynamic recrystallization is accelerated by rise of temperature and drop of strain rate. The critical driving force for DRX increases by rise of strain rate and decrease of temperature [41].

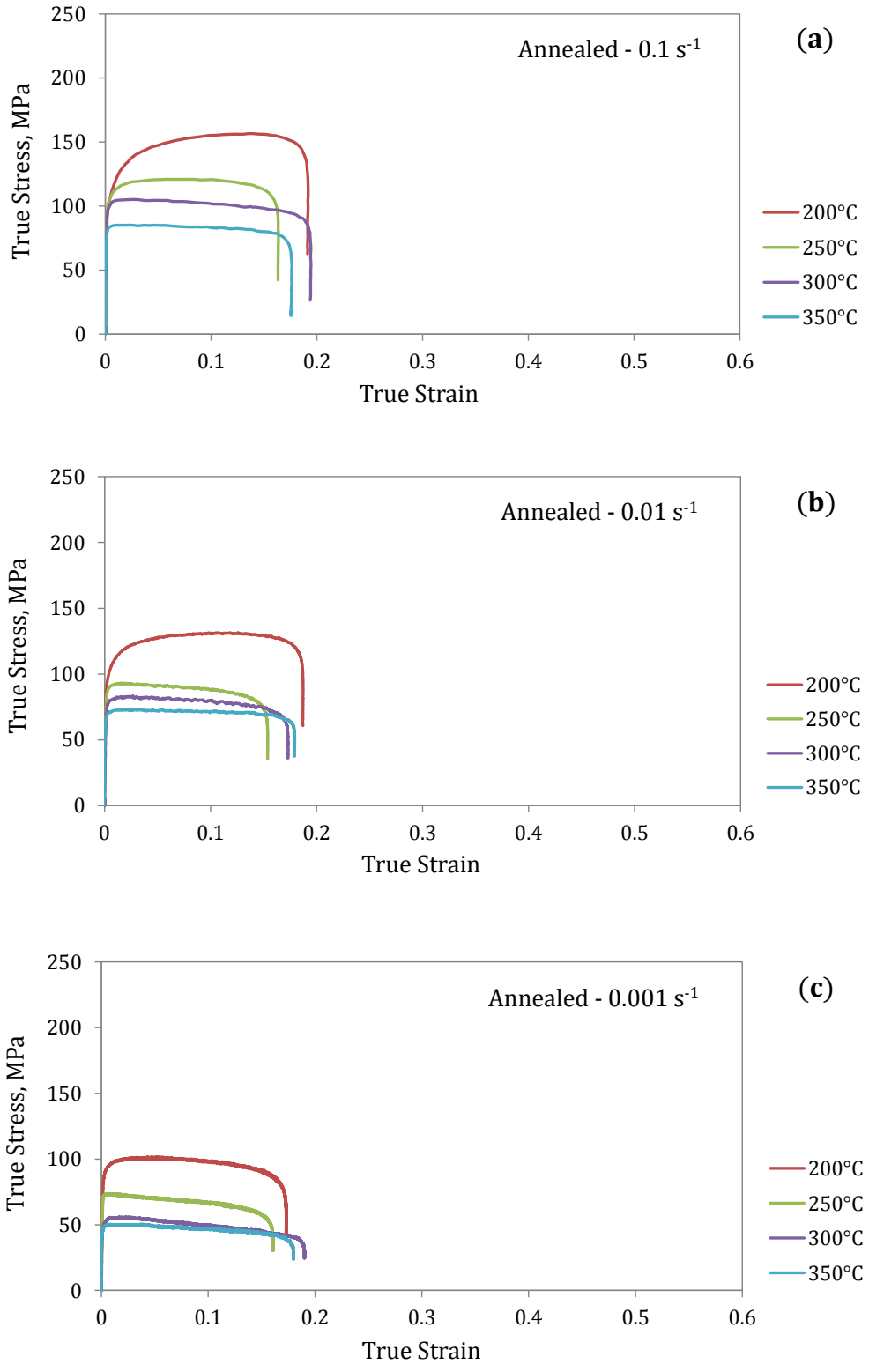

Figure 17: High temperature tensile true stress-true strain curves of the studied Al-Zn-Mg-Cu alloy in annealed condition under the strain rate of: (a) 0.1 s^{-1}, (b) 0.01 s^{-1}, and (c) 0.001 s^{-1}

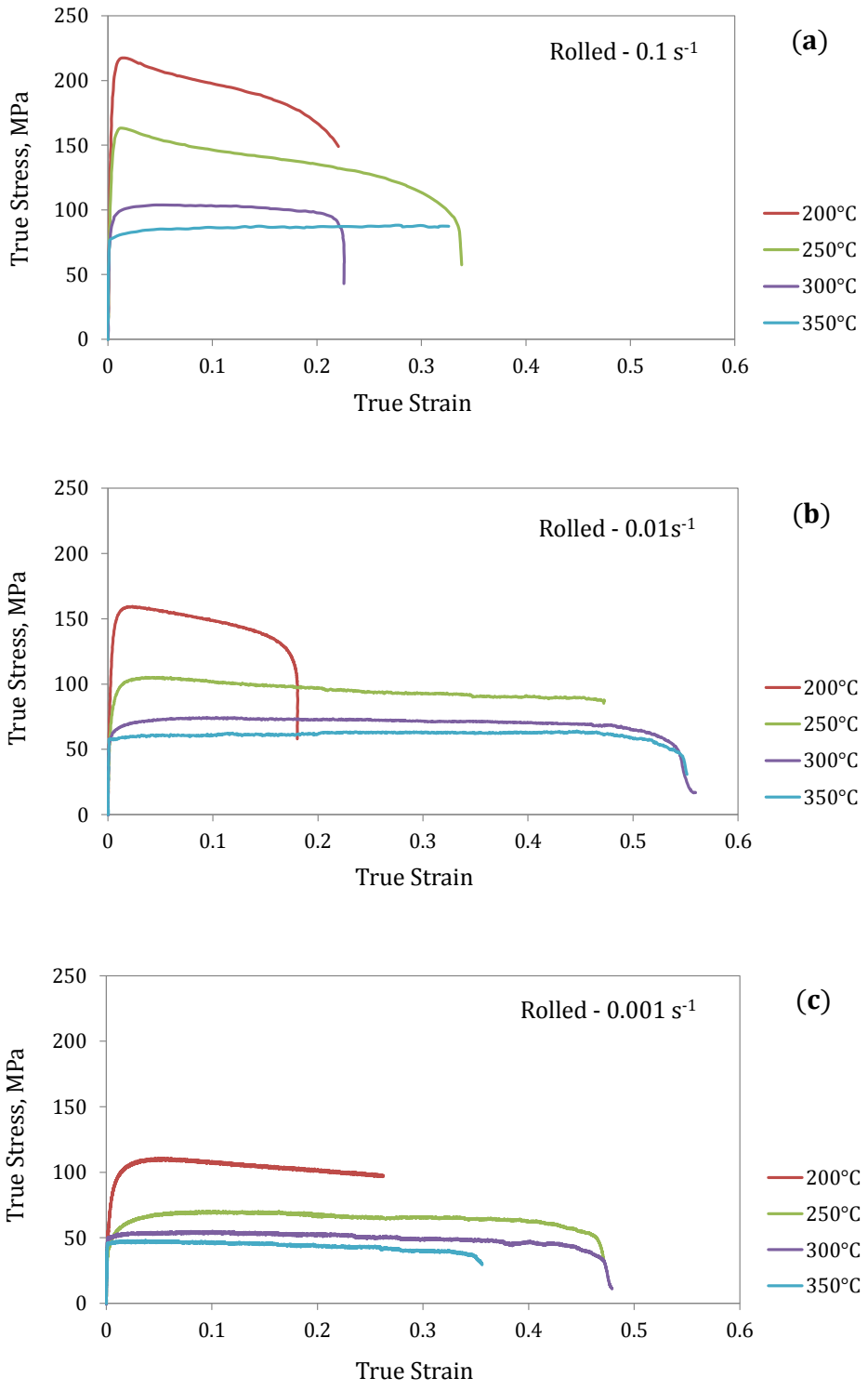

Figure 18: High temperature tensile true stress-true strain curves of the studied Al-Zn-Mg-Cu alloy in rolled condition under the strain rate of: (a) 0.1 s^{-1}, (b) 0.01 s^{-1}, and (c) 0.001 s^{-1}

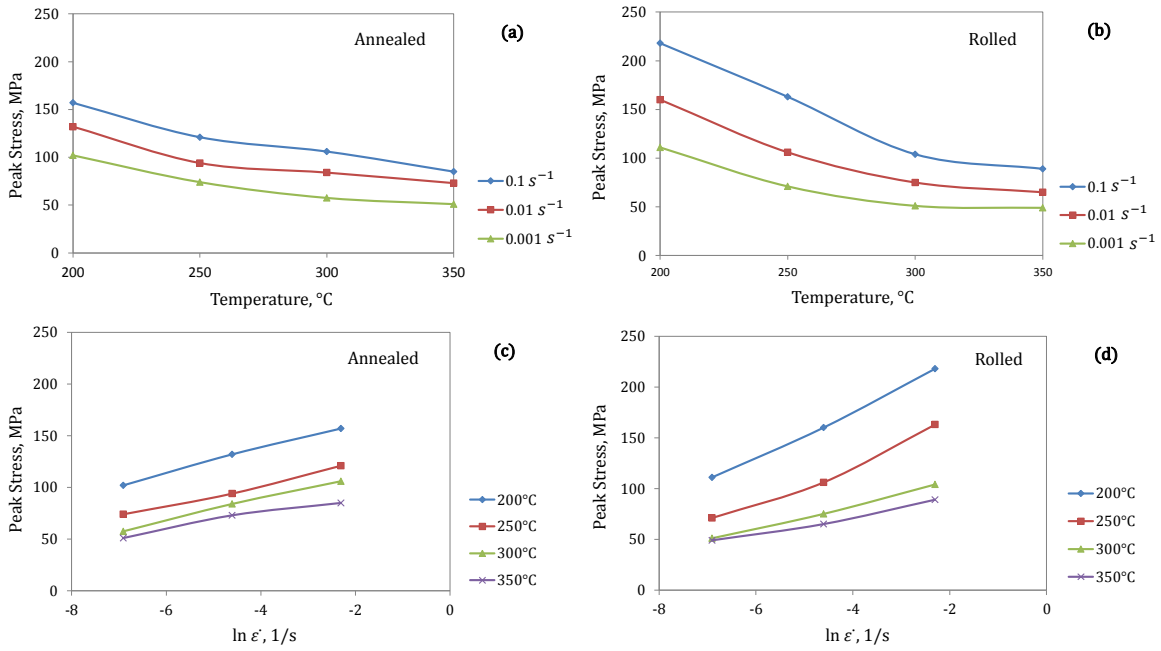

Figure 19: Effects of deformation parameters on the peak stress of (a),(c) annealed (b),(d) rolled Al 7075 samples

Generally, the strain rate sensitivity coefficient (m) represents the transfer and diffusion ability of necking. Plastic deformation capability of a material in hot deformation typically rises with the increase of strain rate sensitivity coefficient [31]. It is generally accepted that the finer microstructure could result in more uniform deformation [32].

$$m = \frac{\partial \ln \sigma}{\partial \ln \dot{\epsilon}} \mid_{\epsilon,T} \tag{1}$$

The variation of the strain rate sensitivity coefficient (m) as a function of strain can be seen in Fig. 20, exhibiting strong dependence to deformation temperature. This can be attributed to temperature dependence of diffusion related mechanisms and resultant rate sensitivity [47]. It is worth noting that strain rate sensitivity shows a considerable increase at 300 °C and 250 °C in annealed and rolled samples, respectively.

In the annealed condition, the strain rate sensitivity values obtained at 300 °C are slightly greater than those obtained at 350 °C for the whole strain interval. A similar behavior was also seen for the rolled condition where m values were higher at 250 °C compared to that of 300 °C and 350 °C.

It is expected that m values rise with the increase of deformation temperature due to thermally activated mechanisms.However, constancy of m can be attributed to the onset of DRX processes which may occur over a range of strain rates and temperatures [48, 49]. In the present case, this constant behavior of m values has been reported after the dominance of DRX around 300 °C for annealed samples and 250 °C for rolled ones which might explain the similar strain rate sensitivity values at both temperatures.

Fig. 21 represents the values of failure elongation as a function of deformation temperature and strain rate for both annealed and rolled samples. Ductility of rolled samples was found to be higher than that of annealed ones. This might be due to grain boundary sliding and migration (GBS/GBM) of rolled samples at elevated temperatures [50]. It has been shown that GBS can be the controlling deformation mechanism when structure of materials is fine and can lead to superplasticity [51]. Cold rolling procedure provides finer structure for aluminum. Therefore, higher levels of ductility are expected to be observed for rolled samples [52].

It can also be seen that annealed specimens do not show considerable variations in elongation values at different deformation temperatures and rates [21]. However, ductility levels of rolled samples are remarkably dependent on both deformation temperatures and strain rates. Ductility of rolled specimen increases with rise of deformation temperature. It could be attributed to occurrence of softening mechanisms at high temperature. It is well-known that DRV and DRX are the possible softening mechanisms for deformation of aluminum alloys at elevated temperature [50]. As straining goes on, necking will be followed by the initiation of some defects such as

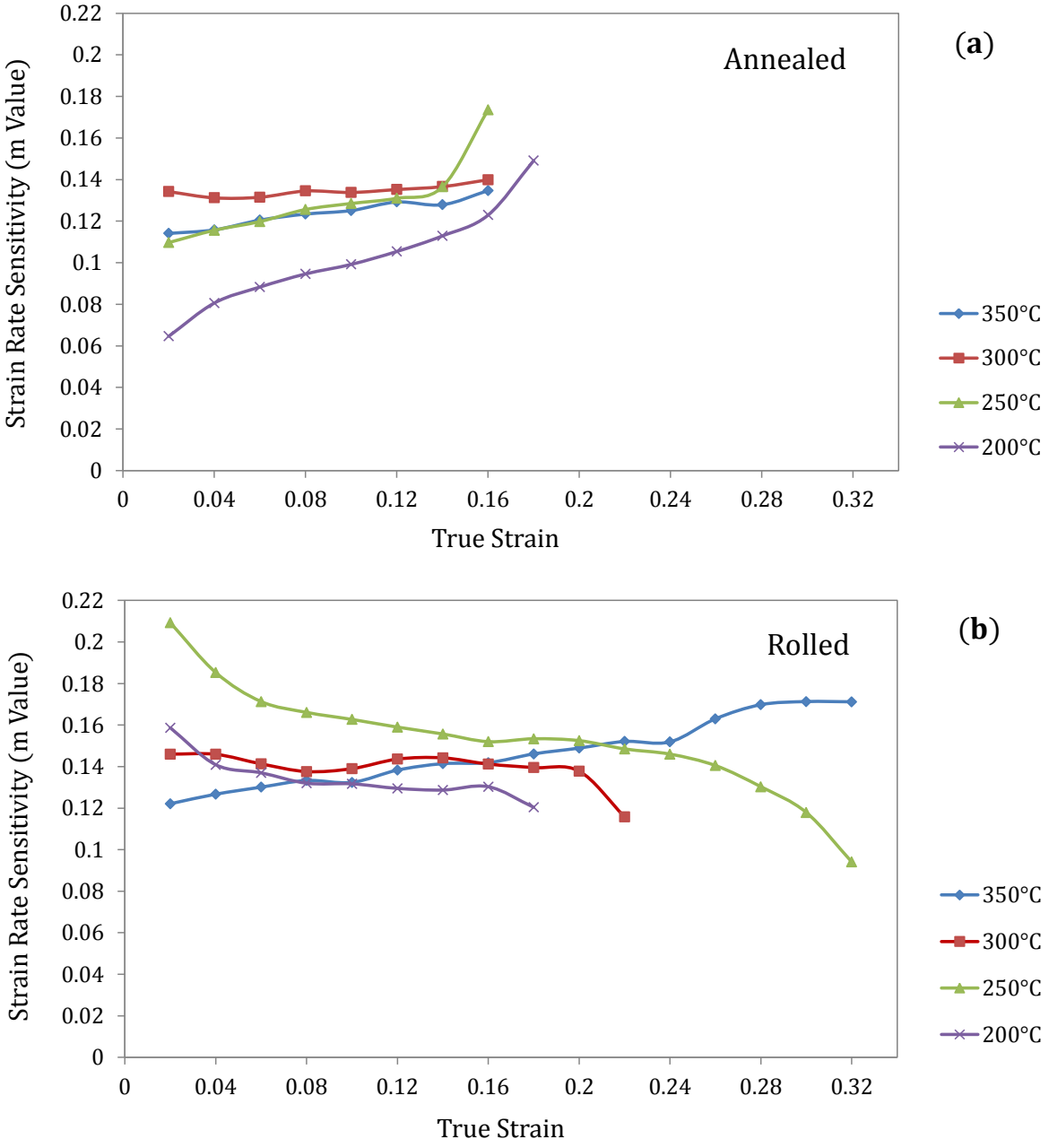

Figure 20: Effect of deformation strain on the strain rate sensitivity coefficient (m) of the (a) annealed and (b) rolled

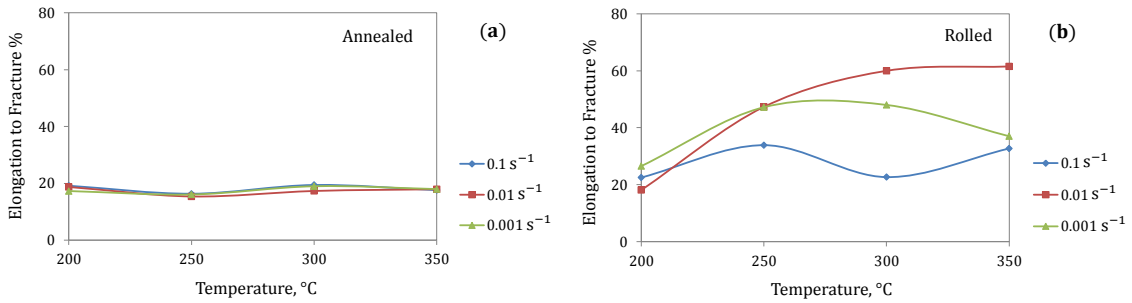

Figure 21: Effects of deformation parameters on the elongation to fracture at (a) annealed and (b) rolled

microvoids and micro cracks due to stress concentration inside of the material.

Conversely, since the flow stress is sensitive to rate of deformation the local deformation slows down. Then by transferring the necking to the weak deformation resistance, the localized necking occurs and the stress level drops promptly in the localized necking stage [28]. In consequence, the hot tensile deformation is a competitive process of work hardening, dynamic softening and the development of voids or cracks [31, 53].

4.2 Microstructural Evolution

The microstructure of as-received as-extruded T651 and annealed conditions are represented in Fig. 22a and b, respectively from the side of sample, perpendicular to the extrusion direction. The microstructure of the as-received alloy consists of deformed and gradually elongated grains (Fig. 22a). Such a parallel and elongated structure can be attributed to the former extrusion processing. As a result of full annealing process conducted to as-received samples, it is evident that grains become coarser and material has transferred to its O-condition (Fig. 22b).

Moreover, micrographs depicting the microstructure of both high temperature annealed and rolled specimens under different deformation temperature and strain rate are shown in Fig. 23 with lower magnification and same samples with higher

magnification in Fig. 24. It can be seen that severe cold work processing leads to a significant refinement in size of the grains and transforms the coarse grained as-received microstructure to one with fine grains after 80% cold work reduction. Whereas, obviously in annealed condition, the elongated coarse grains along the necking zone, has accelerated the propagation of the localized diffusions followed by necking.

Fig. 25, shows the optical micrographs of annealed and rolled conditions to see the difference in fracture necking of two specimens. The microstructure of the starting annealed material depicts layers of grains lying parallel to the extrusion axis. As the rolling strain increases, the grains are elongated in the rolling direction and as a result, the aspect ratio increases. Consequently, it can be seen there is noticeable refining of the grains after applying 80% of cold work to the annealed samples confirmed by tensile deformation.

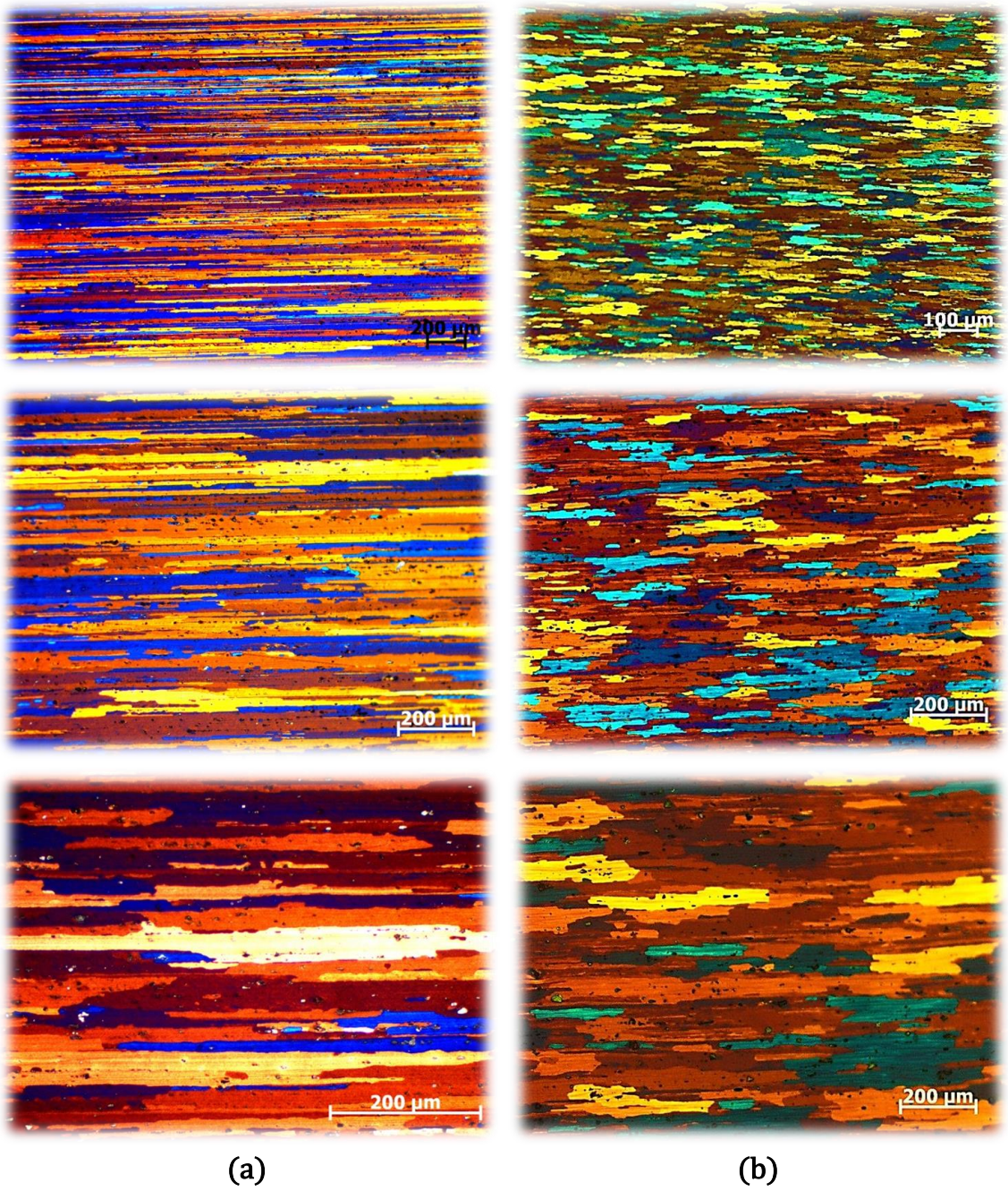

Figure 22: (a) As-received aluminum T651 (b) Full annealed sample

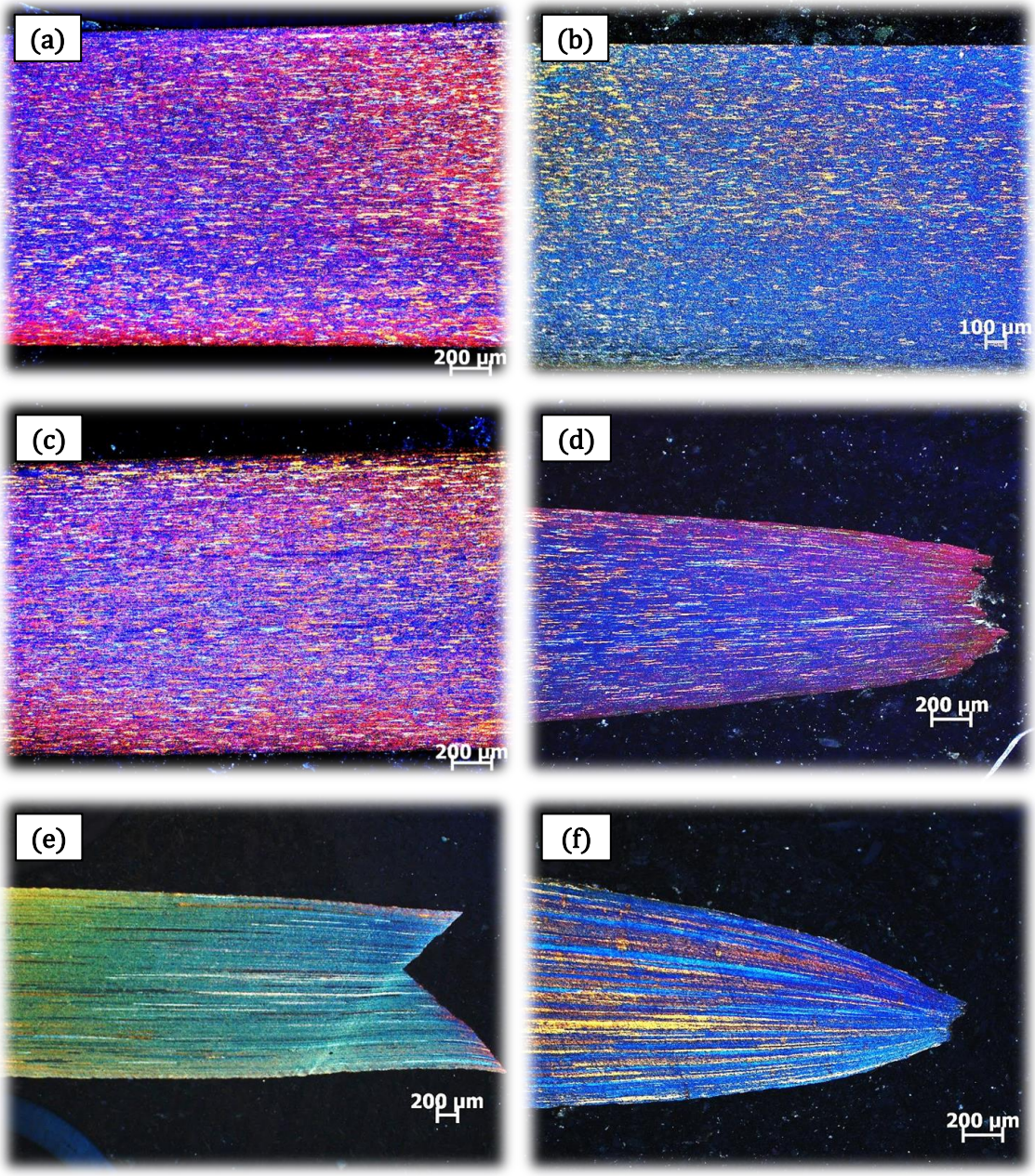

Figure 23: OM images of the fractured specimens with 5x magnification; (a) rolled and tested at 350 °C with strain rate of 0.01 s^{-1}, (b) rolled and tested at 350 °C with strain rate of 0.001 $^{-1}$, (c) rolled and tested at 300 °C with strain rate of 0.01 $^{-1}$, (d) rolled and tested at 300 °C with strain rate of 0.01 $^{-1}$, (e) annealed and tested at ambient temperature with strain rate of 0.01 s^{-1}, (f) annealed and tested at 350 °C with strain rate of 0.01 s^{-1}

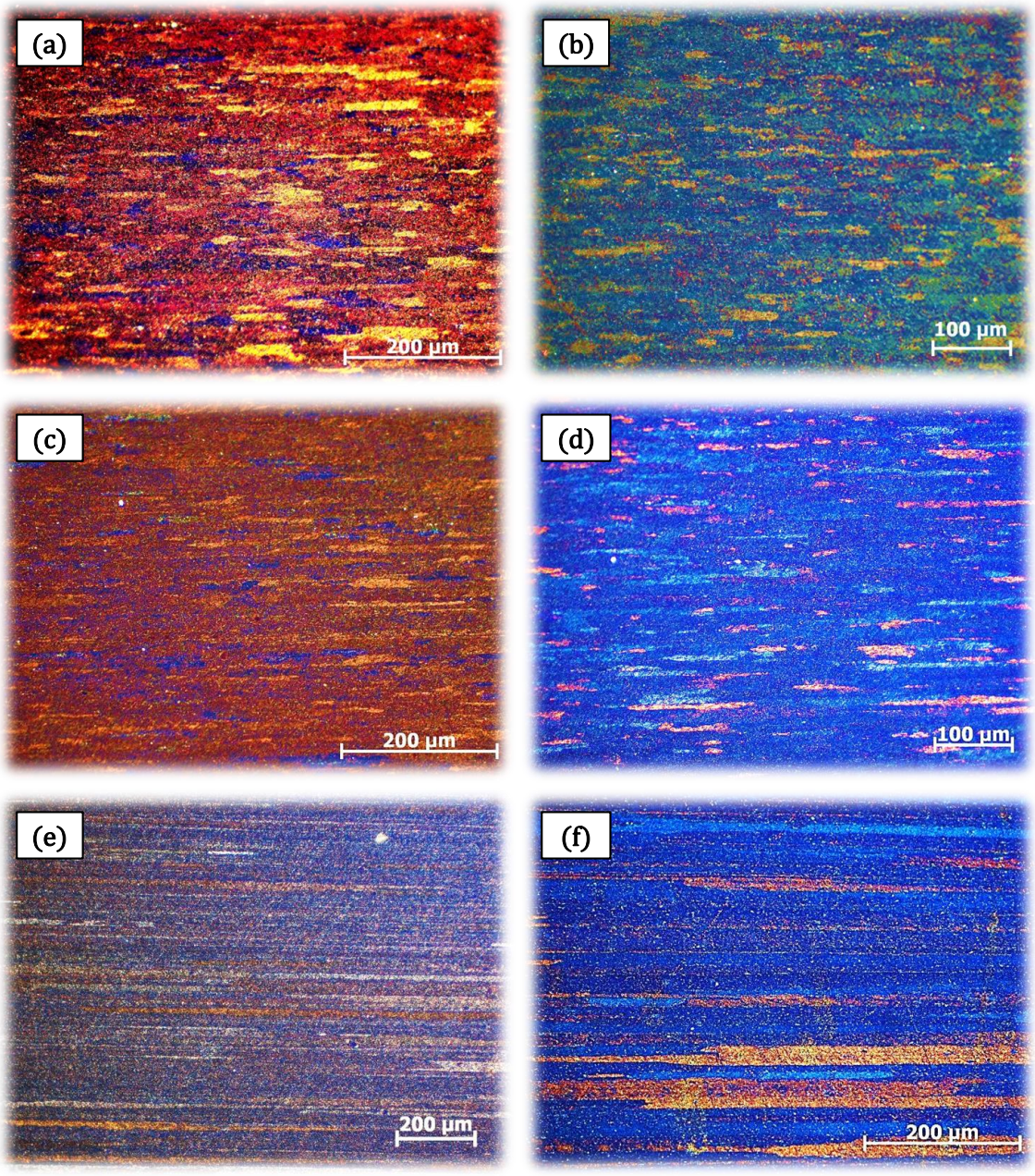

Figure 24: OM images of the fractured specimens with 20x magnification; (a) rolled and tested at 350 °C with strain rate of 0.01 s^{-1}, (b) rolled and tested at 350 °C with strain rate of 0.001 s^{-1}, (c) rolled and tested at 300 °C with strain rate of 0.01 s^{-1}, (d) rolled and tested at 300 °C with strain rate of 0.001 s^{-1}, (e) annealed and tested at ambient temperature with strain rate of 0.01 s^{-1}, (f) annealed and tested at 350 °C with strain rate of 0.01 s^{-1}

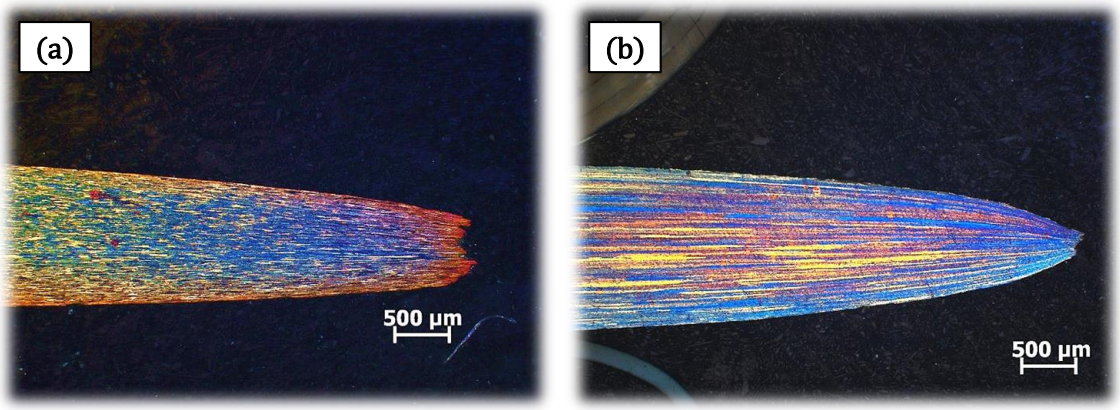

Figure 25: OM images of the fractured specimens with 2.5x magnification; (a) rolled and tested at 300 °C with strain rate of 0.001 $^{-1}$, (b) annealed and tested at 350 °C with strain rate of 0.01 $^{-1}$

4.3 Fracture Morphology Analysis

Coalescence of voids by internal necking is a ubiquitous mechanism of material failure which has been seen mostly on post-mortem section of heavily deformed specimens. This internal necking mechanism is more often to occur at low and moderate stress level including the situations of both tensile and shear loading where in elevated temperatures, this occurrence could be delayed and provides more ductile behavior [54]. Generally, in metallic alloys as straining goes on, the possible phenomenons for emerging the voids are second-phases, weak interfaces, slip-bands or twin intersections, then they become larger and swivel in proportions depending on the stress level and the material type. However, in some materials the growth of the voids are limited such that after actualizing the nucleation, failure is specified via void coalescence [55].

Fracture morphology of different test conditions was observed with SEM and in some cases EDS (Energy Dispersive Spectroscopy) was applied. It is generally evident that the fracture surface of all specimens covered with high amount of equi-axial dimples, tearing edges and micro-voids which are considered to be ductile fracture

mechanisms [28]. The presence of large and deep dimples in the fracture surface of the annealed specimen followed by ambient temperature tensile test in comparison to the rolled one is in good agreement with larger straining of the specimen (Fig. 26-27). However, it is apparent that in the mentioned condition, the size of dimples are not the same and the dimple formation is heterogeneous. In the first type, cavities nucleated from coarse precipitates grow continuously until the voids impinge together. This phenomenon is called void coalescence by internal necking in which the formation of voids and cracks are not uniform [56].

By contrast, in the rolled specimen (Fig. 27) it is also clear that dimples and voids are not identically shaped but they are evidently smaller than the annealed sample. This phenomenon is in good agreement with tensile test results of two samples in which cold working provides higher stress level, in contrast it deteriorates the ductility of the material.

Fig. 28, shows the fracture morphologies of the rolled specimens at all deformation temperatures with three tested strain rates. It is obvious that the sizes of dimples are quite small and the coalescence of dimples can seldomly be observed at relatively low temperatures. It is mainly due to that the internal necking is hard to occur under relatively low deformation temperature, and the deformation is prone to generate some microscopic dimples rather than maximize the previously-implied small ones. As deformation temperature rises,the coalescence of dimples is most likely to happen. Moreover, it can be seen that fracture surface consists of dimples and tearing edges. The intergranular fracture and coalescence of voids seem to be main fracture mechanisms for this sample. It is well-known that the nucleation, growth and coalescence of microvoids lead to final fracture of metallic materials. It is also worth noting that dimples and void sizes rise with drop of strain rate [53].

Fig. 29 represents the fracture surface of both annealed and rolled samples at

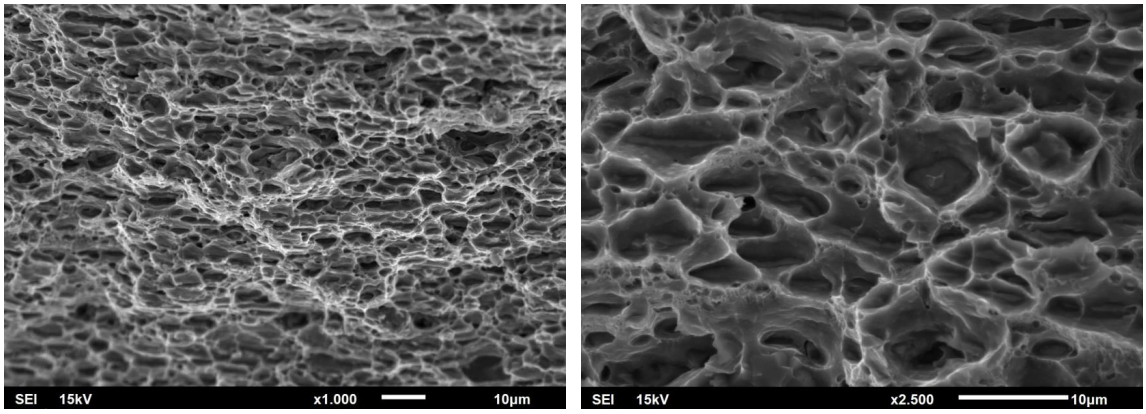

Figure 26: Fracture surface of annealed specimen tested at room temperature with the strain rate of 0.01 s^{-1}

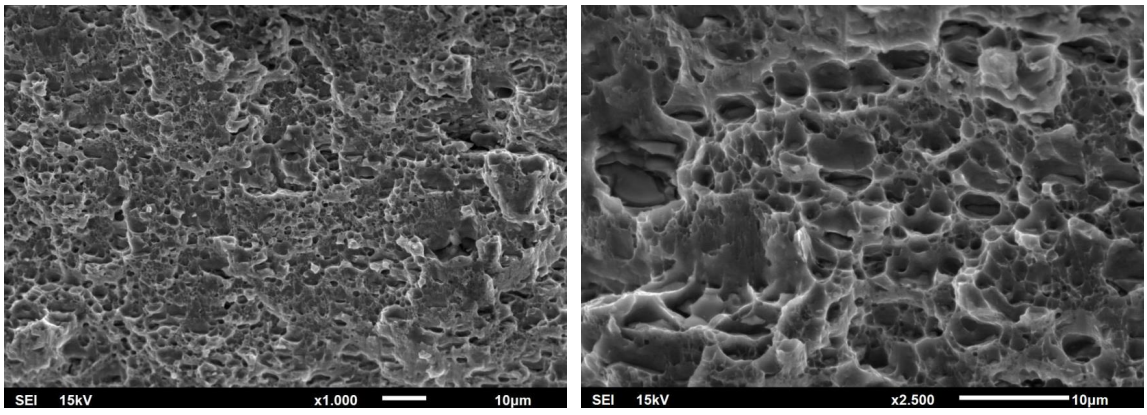

Figure 27: Fracture surface of rolled specimen tested at room temperature with the strain rate of 0.01 s^{-1}

the same deformation temperature of 350 °C under the moderate strain rate. comparatively, a significant rise in the size of dimples and cracks can be observed on the fracture surface of the annealed specimen at 350 °C under the strain rate of 0.01 s^{-1}. However, with comparison to the fracture surface of the rolled samples at 200 °C (Fig. 28), there is a noticeable enlargement in the void sizes at 350 °C due to coalescence of the voids and dimples at relatively high deformation temperature. Moreover, it can be seen that severe cold working increased the uniformity of the well-developed dimples on the fractured surface [28].

The growth and coalescence of dimples can be attributed to the increase of internal necking ability of materials with the decrease of strain rate [28]. Moreover, some newly recrystallized grains are noticed on the fracture surface of 350 °C - 0.001 s^{-1}. Due to the grain boundary sliding (GBS) deformation mechanism in fine recrystallized structure, the intergranular fracture can take place [28].

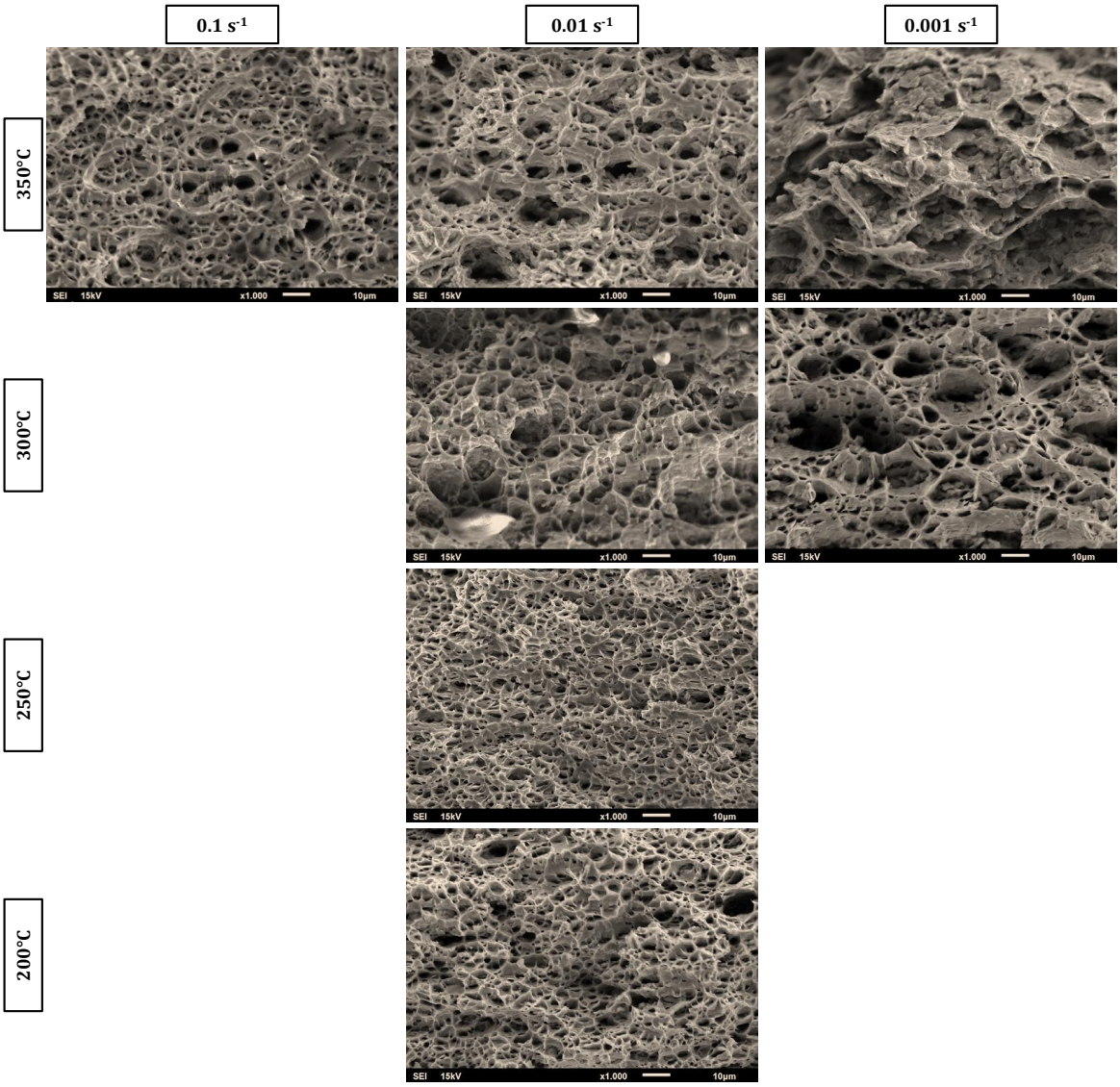

Figure 28: Fracture surface of the rolled specimens tested at elevated temperatures and different strain rates

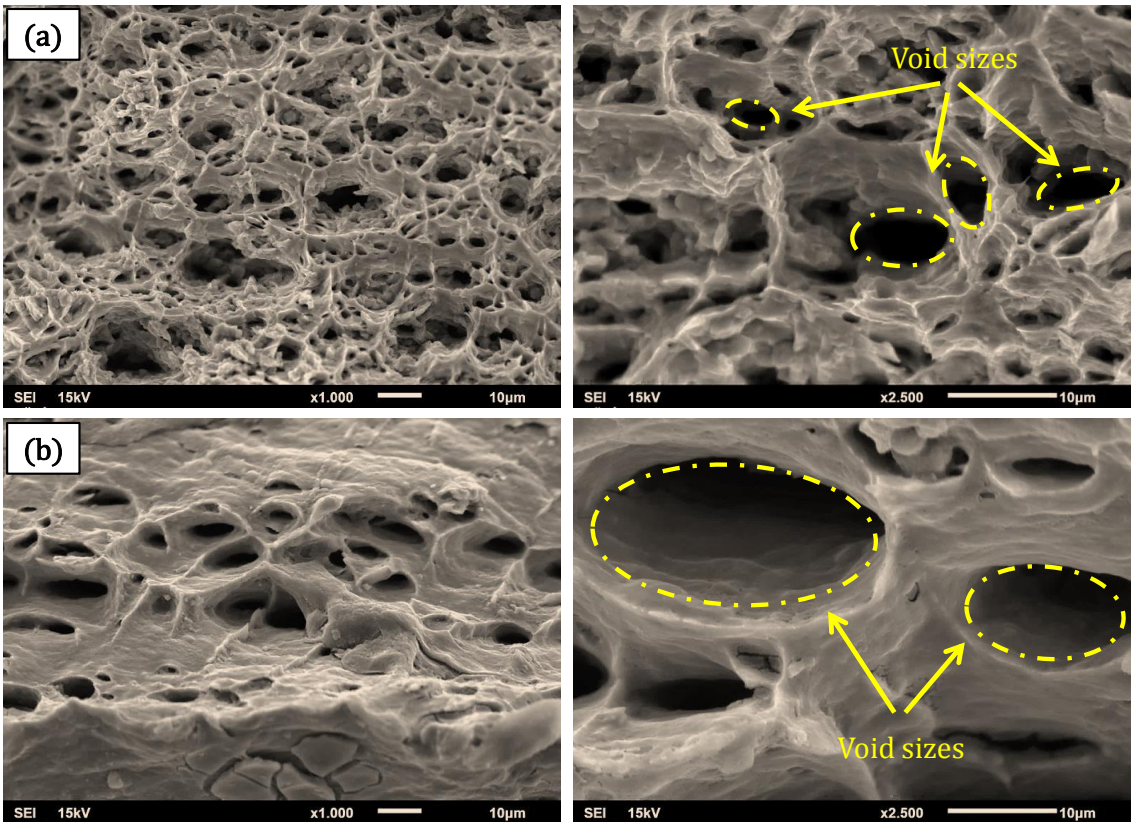

Figure 29: Fractured surface of the (a) rolled samples and (b) annealed samples at the deformation temperature of 350 °C under the strain rate of 0.01 s^{-1}

4.3.1 Effect of Strain Rate on Fracture Morphology and Mechanical Behavior of Cold Rolled Samples

Fig. 30 shows the fracture morphologies at deformation temperature of 350 °C with different strain rates of 0.01 and 0.001 s^{-1}. As shown in Fig. 30 a, b the fracture surface is covered with a massive amount of dimples and tearing edges in which by decreasing the rate of strain, it is obvious that the size of dimples and cracks has increased. This could be referred to the fact that occurrence of internal necking is hard to happen at lower temperatures and high strain rates and respectively by decreasing the strain rate at 350 °C temperature, the coalescence of dimples is most likely to happen. Respectively, a lot of large dimples and cracks can be observed on the fracture surface at 350 °C under the strain rate of 0.001 s^{-1}. In 7075 aluminum alloy, it is well documented that precipitates with various phases may be introduced [57].

Fracture morphology of cold rolled samples followed by tensile test at different strain rates of 0.01 s^{-1} and 0.001 s^{-1} under the constant deformation temperature of 350 °C can be seen in Fig. 30. It is apparent that the size of dimples increased with rise of temperature, however, the number of dimples reduced at higher deformation temperatures because of enlargement of the previously-induced small ones. This behavior can be referred to the coalescence of dimples at 350 °C [28]. It is well-documented that at relatively low deformation temperatures, deformations prefer to induce microscopic dimples, while induced dimples tend to coalescence at higher deformation temperatures [58]. Some equiaxed grains which can be formed as a result of DRX are observed. It is also worth noting that the number of recrystallized grains considerably increased with rise of deformation temperatures [58].

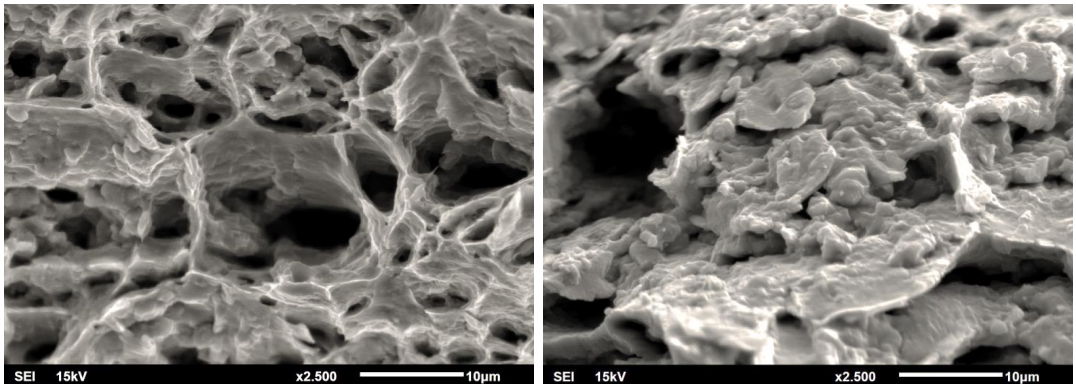

Figure 30: Effect of strain rate on the fracture surface of the rolled samples at 350°C with strain rate of (a) 0.01 s^{-1} (b) 0.001 s^{-1}

4.3.2 Effect of second phase particles and temperature on ductility drop at 350 °C

With regards to the high temperature true stress-strain curves (Fig. 18) of cold rolled samples under the strain rates of 0.01 and 0.001 s^{-1}, it can be seen a small drop in elongation to fracture by rising the deformation temperature from 300 to 350 °C. Fig. 31 demonstrates the energy dispersive spectroscopy (EDS) study on the fracture surface of the cold rolled specimens after high temperature tensile deformation at 300 and 350 °C under the constant strain rate of 0.001 s^{-1}. The EDS result has revealed the formation of Fe-rich secondary phases in the samples which deformed at 350 °C -0.001 s^{-1}.

It is well-known that high deformation temperature and low deformation rate might cause dynamic precipitation during deformation of Al7075 alloy [59]. It was reported that those secondary phases which consists of Fe element could adversely affect ductility of Al7075 alloy [60]. During deformation of Al7075 alloy at 350°C, Taheri-Mandarjani et al. [41] also observed the ductility drop due to dynamic precipitation. The Fe-rich phases are favorite sites for the nucleation and growth of micro cavities and cracks [59]. As a matter of fact, the reason of decreasing elongation to

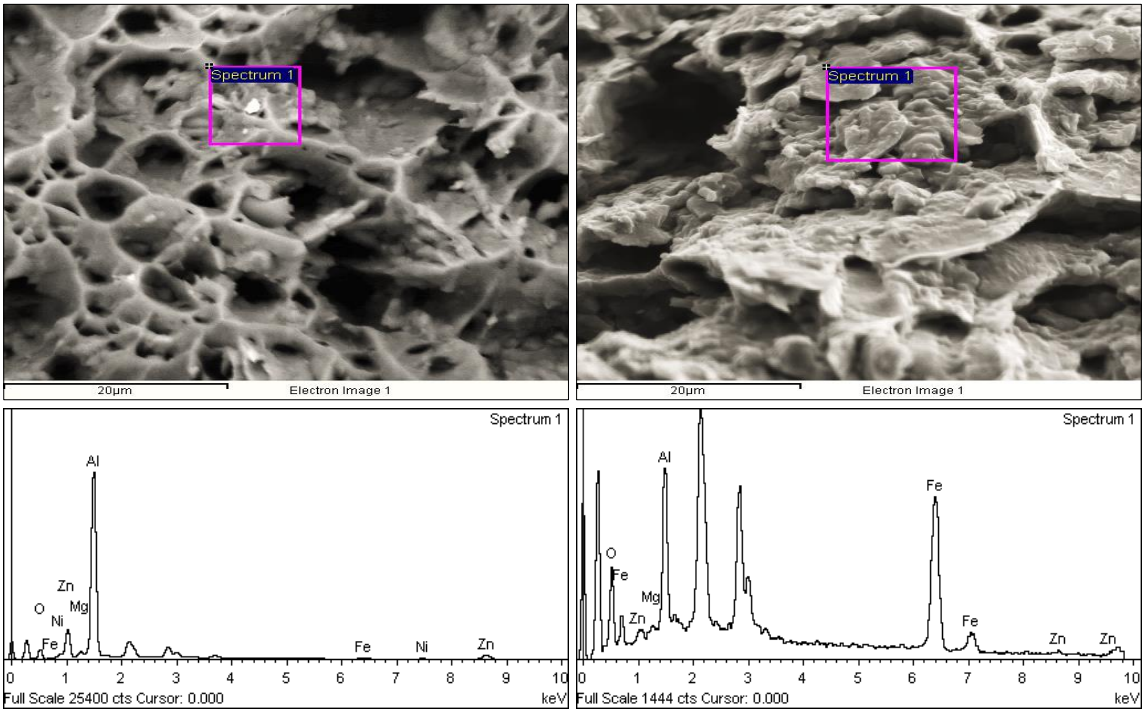

Element	Weight%	Atomic%
O	9.53	17.33
Mg	1.58	1.9
Al	64.42	69.47
Fe	3.22	1.68
Ni	3.28	1.63
Zn	17.97	8
Totals	100	

(a)

Element	Weight%	Atomic%
O	10.13	25.1
Mg	0.79	1.28
Al	13.94	20.48
Fe	73.08	51.88
Zn	2.07	1.25
Totals	100	

(b)

Figure 31: The results of EDS analysis and the related SEM images of the rolled specimens after high temperature tensile test under constant strain rate of 0.001 s^{-1} and deformation temperatures of; (a) 300°C and (b) 350°C

fracture at these brittle sites could be due to nucleation and formation of cavities around the precipitates thereby with further straining at elevated temperatures, increasing the length of these micro cracks and accelerating the early fracture could be the result [41, 59, 60].

Moreover, it has been claimed that formation of the coarse intermetallic particles of Al, Cu and Fe as a second phase particles are important fatigue crack nucleation sites in Al7075-T651 alloy. The fracture morphology of the specimen has been covered by many dimples with precipitant particles which each of them was a brittle zone to initiating the crack. Therefore, the fatigue damage of Al 7075-T651 alloy was initiated by Fe-rich intermetallic particles [66]. Finally, the decrease of elongation value at 350 °C−0.001 s^{-1} can be attributed to the formation of Fe-rich secondary phases which impede dislocation motions.

4.4 Activation Energy Calculation

The concept of thermal activation is related to the thermal vibration of the atoms that even in a solid have a distribution similar to that in a noble gas, and therefore the gas constant, R, has been utilized in the equation. The fraction of atoms above an energy level Q needed for a certain type of jump, like vacancy migration assisting dislocation climb, is given by the Arrhenius term (exp [–Q/RT]). For this study, the Zener-Hollomon parameter in an exponent type equation has been utilized for both tested conditions in order to calculate the activation energy required to initiate the deformation at elevated temperatures for the studied conditions. In hot working processes, several constitutive equations have been applied [61–63], where Z can be determined from:

$$Z = \dot{\epsilon}\ exp(\frac{Q}{RT}) \tag{2}$$

Therefore:

$$\dot{\epsilon} = A\ F(\sigma)\ exp(\frac{-Q}{RT}) \tag{3}$$

Where, $\dot{\epsilon}$ is the strain rate, Q is the apparent activation energy for hot deformation, R is the universal gas constant, T is the absolute temperature, A, and n are material constants. F(σ) is a function of flow stress which can be described as follows:

$$F(\sigma) = A_1\sigma^n \tag{4}$$

$$F(\sigma) = A_2 exp(\beta\sigma) \tag{5}$$

$$F(\sigma) = A_3[sinh(\alpha\sigma)]^n \tag{6}$$

α is a material constant. Substituting function of flow stress ($F(\sigma)$) into Eqn. 3 gives:

$$\dot{\epsilon} = B\ exp(\beta\alpha)\ exp(\frac{-Q}{RT}) \tag{7}$$

$$\dot{\epsilon} = C\ \sigma^n\ exp(\frac{-Q}{RT}) \tag{8}$$

Here B and C are the material constants, taking the logarithm of Eqns. 7 and 8, gives:

$$(\frac{\partial \ln(\dot{\epsilon})}{\partial \ln(\sigma_p)})_T = n \tag{9}$$

$$(\frac{\partial \ln(\dot{\epsilon})}{\partial \sigma_p})_T = \beta \tag{10}$$

Also α and β, which are related to each other through:

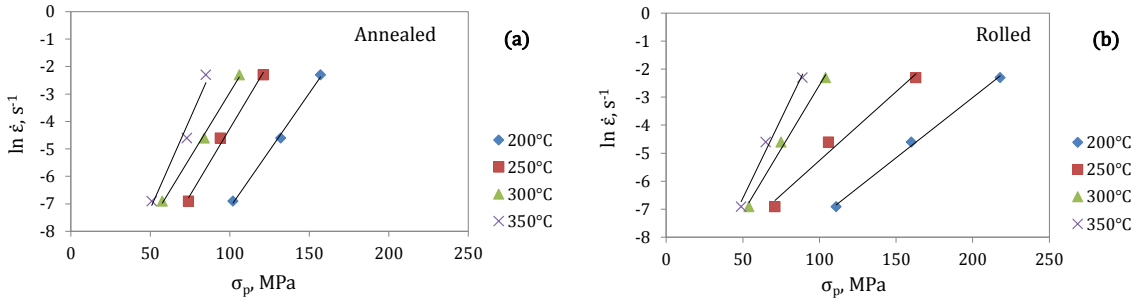

Figure 32: Relation of: $\ln(\sigma_p), MPa$ - $\ln(\dot{\epsilon}), s^{-1}$ (a) annealed, (b) rolled

$$\alpha = \frac{\beta}{n} \tag{11}$$

The values of n and β can be obtained from the slope of the lines plotted according to Eqns. 9 and 10, respectively. As the slopes of lines are similar, the value of n and β can be calculated for different deformation temperatures using linear fitting method. Fig. 32 shows $\ln(\dot{\epsilon})$ versus stress at different temperatures and Fig. 33 represents $\ln(\dot{\epsilon})$ versus $\ln(\sigma)$ at different temperatures. Accordingly, the mean values of n and β can be obtained as 5.9 MPa^{-1} and 0.046 MPa^{-1}. Therefore, α can be computed from n and β as $\alpha = \frac{\beta}{n} = 0.008$. For the given strain rate conditions, Q can be defined as Eqn. 12:

$$Q = nRS \tag{12}$$

Where S is:

$$S = (\frac{d\{\ln[sinh(\alpha\sigma_p)]\}}{d(\frac{1}{T})})_{\dot{\epsilon}} \tag{13}$$

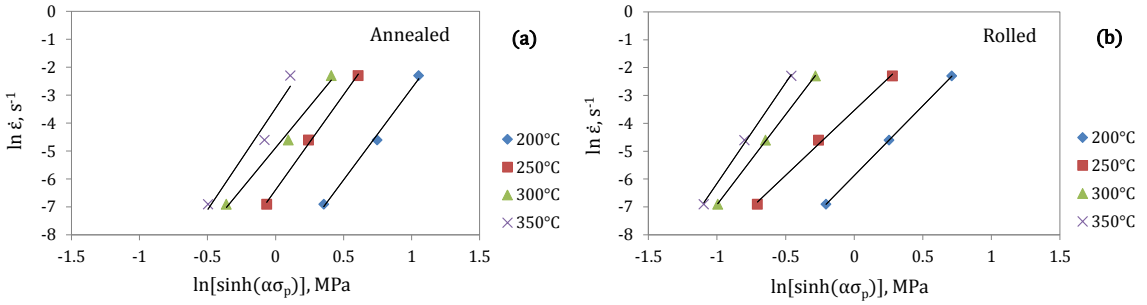

Figure 33: Relation of: $\ln[sinh(\alpha\sigma_p)]$ - $\ln(\dot{\epsilon}), s^{-1}$ (a) annealed, (b) rolled

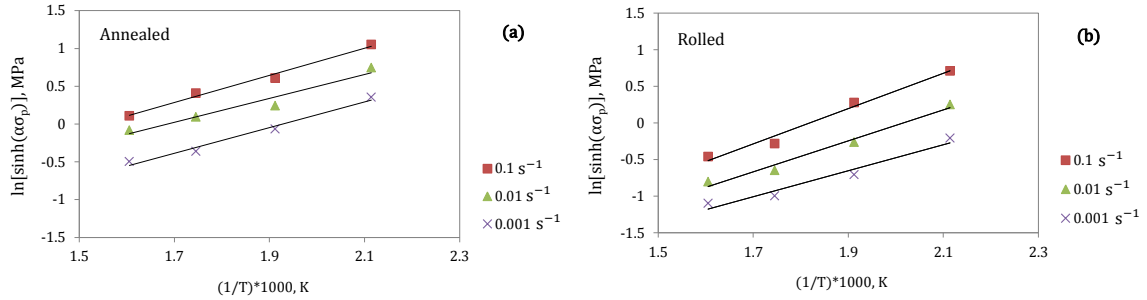

Figure 34: Relation of $(1/T) \times 1000, K$ - $\ln[sinh(\alpha\sigma_p)], MPa$ (a) annealed, (b) rolled

The value of Q can be derived from the line slope of $\ln(\dot{\epsilon})$ versus $\ln[sinh(\alpha\sigma_p)]$ and $\ln[sinh(\alpha\sigma_p)]$ versus $\frac{1}{T}$ plots. From the group of parallel lines in Fig. 34, the mean values of Q for annealed samples and rolled samples were calculated to be 93 $^{kJ}/_{mol}$ and 106 $^{kJ}/_{mol}$, respectively.

According to the mean values of Q, it can also be found that rolled samples required more energy to be deformed at examined temperatures. This may be attributed to the finer and elongated structure of rolled specimen [64, 65].

CHAPTER V

CONCLUSION

In the present work, the high temperature tensile tests of the annealed and severely cold worked of an Al-Zn-Mg-Cu alloy in both ambient and elevated temperatures were carried out to characterize the deformation mechanisms. The experimental data of tensile behaviors, microstructural evolution and fracture morphology were analyzed. According to the tensile test results of the studied alloy in the mentioned conditions, a general trend of forming process at room and high temperatures can be suggested. Generally, there are two main parameters that can affect the forming process, deformation temperature and rate.

It has been found that in order to use this material for the purpose of cold forming, it is advised that using the O-tempered condition with the strain rate of 0.001 s^{-1} could enhance the formability. Whereas complex surfaces with sharp edges and curves where hot forming is preferable to cold forming, severely rolled condition could be the case. It has been observed that, fine structure of material obtained by cold work, leads to significant formability at 350 °C under the strain rate of 0.01 s^{-1}. Moreover, some important conclusions can be made as follows:

- The elongation to fracture of the studied Al-Zn-Mg-Cu alloy increases with the increase of deformation temperature. As temperature rises, owing to activating of softening mechanism the yield strength values of both annealed and rolled specimens remarkably decreases.

- The flow behaviors of the studied aluminum alloy are significantly affected by the deformation temperature and strain rate. Although, in both annealed and rolled conditions at room temperature the effect of strain rate is negligible.

- The rolled material shows a significant ductile behavior under the deformation temperature of 350 °C and remarkable strain hardening at 200 °C, while in the annealed condition temperature doesn't play a significant role on elongation of the material.

- Due to the formation of fine grains after cold working, there is a significant rise in peak stress at room temperature, while coarse grains in annealed condition has provided a notable ductility.

- Lower ductility behavior was noticed at 350 °C with strain rate of 0.001 s^{-1} which may be attributed to the formation of Fe-rich secondary phase. In the rolled samples by initiating DRX at elevated temperature and activating the softening mechanisms, it has been observed that increasing the strain rate can raise the peak stresses more than annealed ones.

- From the observations on the rolled fracture surfaces, the growth of dimples and micro-voids are more evident at lower deformation rate since this can provide longer time to coalescence and help the microvoids linkage by internal necking. Also, by increasing the deformation temperature because of having higher diffusion rate, voids coalescence is easier to occur.

CHAPTER VI

RECOMMENDATIONS AND FUTURE STUDY

Within the engaged research that has been undertaken for this thesis, some remarkable topics has have been highlighted, on which further research would be beneficial. As mentioned earlier, heating and cooling operations that are carried out for the purpose of changing the mechanical properties, metallurgical structure, and the residual stress state of a metallic specimen, in its broadest sense is known as heat treatment process.

Specifically speaking of aluminum alloys, however, its usage is commonly limited to the operations employed to increase strength and hardness of the precipitation-hardenable wrought and cast alloys, which are referred to as "heat-treatable" alloys. On the other hand, "non-heat-treatable" alloys, depend primarily on cold work to increase strength. With regards to the studied material, which is categorized as a heat treatable alloy, there is a big potential for characterizing the behavior of this material after artificially aging followed by severely cold work.

For static aging there would be two effective parameters; aging temperature and duration, which according to the material behavior, optimum condition needs to be specified after periodic tests.

In aluminum heat treatment, this process is called T8 tempering. This process consists of steps as solution heat treating, cold working followed by artificially aging. Respectively one essential attribute of a precipitation-hardening alloy system is a temperature-dependent equilibrium solid solubility, characterized by increasing solubility with increasing temperature.

This investigation could be handsomely completed via performing comparative

high temperature tensile tests between below conditions:

- Severely cold-worked sample tested at 350 °C (currently known as highest ductility)
- Severely cold-worked followed by static aging at various temperatures and durations.

Bibliography

[1] A. Woodward, "The rolling of aluminium–the process and the products," *TALAT Lecture*, vol. 1301, 1994.

[2] H. McQueen, "Metal forming: Industrial, mechanical computational and microstructural," *Journal of Materials Processing Technology*, vol. 37, no. 1, pp. 3–36, 1993.

[3] D. Dumont, A. Deschamps, and Y. Brechet, "On the relationship between microstructure, strength and toughness in aa7050 aluminum alloy," *Materials Science and Engineering: A*, vol. 356, no. 1, pp. 326–336, 2003.

[4] N. Deshpande, A. Gokhale, D. Denzer, and J. Liu, "Relationship between fracture toughness, fracture path, and microstructure of 7050 aluminum alloy: Part i. quantitative characterization," *Metallurgical and Materials Transactions A*, vol. 29, no. 4, pp. 1191–1201, 1998.

[5] A. Heinz, A. Haszler, C. Keidel, S. Moldenhauer, R. Benedictus, and W. Miller, "Recent development in aluminium alloys for aerospace applications," *Materials Science and Engineering: A*, vol. 280, no. 1, pp. 102–107, 2000.

[6] E. Starke and J. Staley, "Application of modern aluminum alloys to aircraft," *Progress in Aerospace Sciences*, vol. 32, no. 2, pp. 131–172, 1996.

[7] J. C. Williams and E. A. Starke, "Progress in structural materials for aerospace systems," *Acta Materialia*, vol. 51, no. 19, pp. 5775–5799, 2003.

[8] J. Wloka, T. Hack, and S. Virtanen, "Influence of temper and surface condition on the exfoliation behaviour of high strength al–zn–mg–cu alloys," *Corrosion science*, vol. 49, no. 3, pp. 1437–1449, 2007.

[9] K.-k. Chow, *Hot deformation behavior of coarse-grained 5052 aluminum alloy*. PhD thesis, The Hong Kong Polytechnic University, 2001.

[10] H. J. McQueen, S. Spigarelli, M. E. Kassner, and E. Evangelista, *Hot deformation and processing of aluminum alloys*. 2011.

[11] J. E. Hatch, A. Association, *et al.*, *Aluminum: properties and physical metallurgy*. ASM International, 1984.

[12] P. Olafsson, R. Sandstrom, and Å. Karlsson, "Comparison of experimental, calculated and observed values for electrical and thermal conductivity of aluminium alloys," *Journal of materials science*, vol. 32, no. 16, pp. 4383–4390, 1997.

[13] J. V. Thompson, *Alumina-simple chemistry-complex plants*, vol. 196. Maclean Hunter publishing corp 29 north Wacker drive, Chicago, IL 60606, 1995.

[14] I. Aluminum Association, *Rolling aluminum: from the mine through the mill*. Aluminum Association, 1990.

[15] W. F. Smith and J. Hashemi, *Foundations of materials science and engineering*. Mcgraw-Hill Publishing, 2006.

[16] J. R. Davis, J. R. Davis, *et al.*, "Aluminum and aluminum alloys," 1993.

[17] E. P. DeGarmo, J. Black, R. A. Kohser, and B. E. Klamecki, "Materials and process in manufacturing," *Jolm Wiley and Sons, USA*, p. 974, 2003.

[18] A. Korhonen, *On the Work-Hardening of AA 3104-H19 Aluminum Alloy*, vol. 22. Springer, 2013.

[19] J. G. Kaufman, "Introduction to aluminum alloys and tempers," 2000.

[20] I. J. Polmear, "Light alloys- metallurgy of the light metals//((book))," *London and New York, Edward Arnold, 1989, 288*, 1989.

[21] J. G. Avery, "Design manual for impact damage tolerant aircraft structure," 1981.

[22] S. Gourdet and F. Montheillet, "A model of continuous dynamic recrystallization," *Acta Materialia*, vol. 51, no. 9, pp. 2685–2699, 2003.

[23] A. Dehghan-Manshadi, M. R. Barnett, and P. Hodgson, "Recrystallization in aisi 304 austenitic stainless steel during and after hot deformation," *Materials Science and Engineering: A*, vol. 485, no. 1, pp. 664–672, 2008.

[24] K. Stüwe, "Thermal buffering effects at the solidus. implications for the equilibration of partially melted metamorphic rocks," *Tectonophysics*, vol. 248, no. 1, pp. 39–51, 1995.

[25] H. McQueen, W. Wong, and J. Jonas, "Deformation of aluminium at high temperatures and strain rates," *Canadian Journal of Physics*, vol. 45, no. 2, pp. 1225–1234, 1967.

[26] C. Campbell, L. Bendersky, W. Boettinger, and R. Ivester, "Microstructural characterization of al-7075-t651 chips and work pieces produced by high-speed machining," *Materials Science and Engineering: A*, vol. 430, no. 1, pp. 15–26, 2006.

[27] M. Tajally, Z. Huda, and H. Masjuki, "A comparative analysis of tensile and impact-toughness behavior of cold-worked and annealed 7075 aluminum alloy," *International Journal of Impact Engineering*, vol. 37, no. 4, pp. 425–432, 2010.

[28] M. Zhou, Y. Lin, J. Deng, and Y.-Q. Jiang, "Hot tensile deformation behaviors and constitutive model of an al–zn–mg–cu alloy," *Materials & Design*, vol. 59, pp. 141–150, 2014.

[29] Y. Lin, L.-T. Li, Y.-X. Fu, and Y.-Q. Jiang, "Hot compressive deformation behavior of 7075 al alloy under elevated temperature," *Journal of Materials Science*, vol. 47, no. 3, pp. 1306–1318, 2012.

[30] Y. Lin, M.-S. Chen, and J. Zhong, "Prediction of 42crmo steel flow stress at high temperature and strain rate," *Mechanics Research Communications*, vol. 35, no. 3, pp. 142–150, 2008.

[31] Y. Lin, J. Deng, Y.-Q. Jiang, D.-X. Wen, and G. Liu, "Effects of initial δ phase on hot tensile deformation behaviors and fracture characteristics of a typical ni-based superalloy," *Materials Science and Engineering: A*, vol. 598, pp. 251–262, 2014.

[32] N. Chandra, "Constitutive behavior of superplastic materials," *International journal of non-linear mechanics*, vol. 37, no. 3, pp. 461–484, 2002.

[33] H. McQueen and D. Bourell, *Hot workability of metals and alloys*, vol. 39. Springer, 1987.

[34] G. E. Totten and D. S. MacKenzie, "Handbook of aluminum: Vol. 1: Physical metallurgy and processes," vol. 1, 2003.

[35] A. Wusatowska-Sarnek, H. Miura, and T. Sakai, "Nucleation and microtexture development under dynamic recrystallization of copper," *Materials Science and Engineering: A*, vol. 323, no. 1, pp. 177–186, 2002.

[36] X. Huang and Q. Liu, "Determination of crystallographic and macroscopic orientation of planar structures in tem," *Ultramicroscopy*, vol. 74, no. 3, pp. 123–130, 1998.

[37] X. Kai, C. Chen, X. Sun, C. Wang, and Y. Zhao, "Hot deformation behavior and optimization of processing parameters of a typical high-strength al–mg–si alloy," *Materials & Design*, vol. 90, pp. 1151–1158, 2016.

[38] L. Saravanan and T. Senthilvelan, "Investigations on the hot workability characteristics and deformation mechanisms of aluminium alloy-al 2 o 3 nanocomposite," *Materials & Design*, vol. 79, pp. 6–14, 2015.

[39] A. Eivani and A. K. Taheri, "Modeling age hardening kinetics of an al–mg–si–cu aluminum alloy," *journal of materials processing technology*, vol. 205, no. 1, pp. 388–393, 2008.

[40] M. El Mehtedi, F. Musharavati, and S. Spigarelli, "Modelling of the flow behaviour of wrought aluminium alloys at elevated temperatures by a new constitutive equation," *Materials & Design*, vol. 54, pp. 869–873, 2014.

[41] M. Taheri-Mandarjani, A. Zarei-Hanzaki, and H. Abedi, "Hot ductility behavior of an extruded 7075 aluminum alloy," *Materials Science and Engineering: A*, vol. 637, pp. 107–122, 2015.

[42] M. M. Avedesian, H. Baker, *et al.*, *ASM specialty handbook: magnesium and magnesium alloys*. ASM international, 1999.

[43] S. Lauvdal, "Experimental studies of cold roll bonded aluminum alloys," 2011.

[44] S. V. Sajadifar and G. G. Yapici, "Workability characteristics and mechanical behavior modeling of severely deformed pure titanium at high temperatures," *Materials & Design*, vol. 53, pp. 749–757, 2014.

[45] R. Barto and L. Ebert, "Deformation stress state effects on the recrystallization kinetics of molybdenum," *Metallurgical Transactions*, vol. 2, no. 6, pp. 1643–1649, 1971.

[46] C. Shi, W. Mao, and X.-G. Chen, "Evolution of activation energy during hot deformation of aa7150 aluminum alloy," *Materials Science and Engineering: A*, vol. 571, pp. 83–91, 2013.

[47] S. Sajadifar, M. Ketabchi, and B. Bemanizadeh, "Dynamic recrystallization behavior and hot deformation characteristics in 4340 steel," *Metallurgist*, vol. 56, no. 3-4, pp. 310–320, 2012.

[48] E. Poliak and J. Jonas, "A one-parameter approach to determining the critical conditions for the initiation of dynamic recrystallization," *Acta Materialia*, vol. 44, no. 1, pp. 127–136, 1996.

[49] B. Paul, A. Sarkar, J. Chakravartty, A. Verma, R. Kapoor, A. Bidaye, I. Sharma, and A. Suri, "Dynamic recrystallization in sintered cobalt during high-temperature deformation," *Metallurgical and Materials Transactions A*, vol. 41, no. 6, pp. 1474–1482, 2010.

[50] A. Khamei, K. Dehghani, and R. Mahmudi, "Modeling the hot ductility of aa6061 aluminum alloy after severe plastic deformation," *JOM*, vol. 67, no. 5, pp. 966–972, 2015.

[51] L. Li, W. Wei, Y. Lin, C. Lijia, and L. Zheng, "Grain boundary sliding and accommodation mechanisms during superplastic deformation of zk40 alloy processed by ecap," *Journal of materials science*, vol. 41, no. 2, pp. 409–415, 2006.

[52] T. Huang, Q. Dong, X. Gong, N. Hansen, Q. Liu, and X. Huang, "Cold rolled nanostructured super-pure al (99.9996%) containing 1% si particles: structure and strength," *Journal of Materials Science*, vol. 47, no. 22, pp. 7914–7920, 2012.

[53] J. Deng, Y. Lin, S.-S. Li, J. Chen, and Y. Ding, "Hot tensile deformation and fracture behaviors of az31 magnesium alloy," *Materials & Design*, vol. 49, pp. 209–219, 2013.

[54] L. Morin, J.-B. Leblond, and A. A. Benzerga, "Coalescence of voids by internal necking: theoretical estimates and numerical results," *Journal of the Mechanics and Physics of Solids*, vol. 75, pp. 140–158, 2015.

[55] K. Madou, J.-B. Leblond, and L. Morin, "Numerical studies of porous ductile materials containing arbitrary ellipsoidal voids–ii: Evolution of the length and orientation of the void axes," *European Journal of Mechanics-A/Solids*, vol. 42, pp. 490–507, 2013.

[56] Y. Shi, P. Wu, D. Lloyd, and J. Embury, "Crystal plasticity based analysis of localized necking in aluminum tube under internal pressure," *European Journal of Mechanics-A/Solids*, vol. 29, no. 4, pp. 475–483, 2010.

[57] M. Kamiya and T. Yakou, "Role of second-phase particles in chip breakability in aluminum alloys," *International Journal of Machine Tools and Manufacture*, vol. 48, no. 6, pp. 688–697, 2008.

[58] S. Spigarelli, E. Evangelista, and H. McQueen, "Study of hot workability of a heat treated aa6082 aluminum alloy," *Scripta Materialia*, vol. 49, no. 2, pp. 179–183, 2003.

[59] Y. Lin, Y.-Q. Jiang, X.-M. Chen, D.-X. Wen, and H.-M. Zhou, "Effect of creep-aging on precipitates of 7075 aluminum alloy," *Materials Science and Engineering: A*, vol. 588, pp. 347–356, 2013.

[60] A. Abolhasani, A. Zarei-Hanzaki, H. Abedi, and M. Rokni, "The room temperature mechanical properties of hot rolled 7075 aluminum alloy," *Materials & Design*, vol. 34, pp. 631–636, 2012.

[61] S. Sajadifar, G. Yapici, M. Ketabchi, and B. Bemanizadeh, "High temperature deformation behavior of 4340 steel: activation energy calculation and modeling

of flow response," *Journal of Iron and Steel Research, International*, vol. 20, no. 12, pp. 133–139, 2013.

[62] F. Bai, P. Cizek, E. J. Palmiere, and M. W. Rainforth, "Characteristics of the deformed and recrystallised grains obtained after hot plane strain compression of a model fe-30wt% ni alloy," vol. 467, pp. 21–26, 2004.

[63] C. Sellars and G. Davies, "Hot working and forming processes," 1979.

[64] E. L. Dreizin, "Experimental study of stages in aluminium particle combustion in air," *Combustion and Flame*, vol. 105, no. 4, pp. 541–556, 1996.

[65] E. Cerri, E. Evangelista, A. Forcellese, and H. McQueen, "Comparative hot workability of 7012 and 7075 alloys after different pretreatments," *Materials Science and Engineering: A*, vol. 197, no. 2, pp. 181–198, 1995.

[66] Y. Xue, H. El Kadiri, M. Horstemeyer, J. Jordon, and H. Weiland, "Micromechanisms of multistage fatigue crack growth in a high-strength aluminum alloy," *Acta Materialia*, vol. 55, no. 6, pp. 1975–1984, 2007.

VITA

Kambiz Shojaei was born in 1988 in Tehran. He received his B.Sc. degree in machine tools and solid design in Mechanical Engineering from Azad University of Tehran - South Branch in 2012. During the last two years of his bachelor degree and one year after his graduation, he was working in industrial companies as a mechanical designer. In February, 2013, he started his M.Sc. degree in the Graduate School of Engineering at Ozyegin University in Istanbul. During graduate studies, he worked as a teaching assistant and carried out research in Memfis group. His main research interests are in advanced materials-manufacturing and mechanical design. His graduate work focused on the thermomechanical behavior of advanced high strength aluminum alloys.